A NOVEL HYBRID SCAFFOLD FOR MANAGING CRITICAL SIZE MANDIBULAR DEFECTS

by

Sait Emre DOĞAN

M.S., in Dentistry, Necmettin Erbakan University, 2019

Submitted to the Institute of Biomedical Engineering
in partial fulfillment of the requirements
for the degree of
Master of Science
in
Biomedical Engineering

Boğaziçi University
2024

A NOVEL HYBRID SCAFFOLD FOR MANAGING CRITICAL SIZE MANDIBULAR DEFECTS

APPROVED BY:

Prof. Dr. Cengizhan ÖZTÜRK .....
(Thesis Advisor)

Prof.Dr. Bahattin KOÇ .....
(Thesis Co-advisor)

Albert GÜVENİŞ .....

Bora GARİPCAN .....

Duygu EGE .....

DATE OF APPROVAL: 25 December 2023

ACKNOWLEDGMENTS

I would like to express my sincere thanks to my advisors Cengizhan ÖZTÜRK and Bahattin KOÇ, for allowing me to gain independence to work on what I desire in the academic field. I also cannot forget the major help from Cerrahpaşa CAST staff, Tinus Technologies, and Bloocell staff.

I am obliged to thank my brother Abdullah Furkan Doğan for all his support before and during my academic journey and for allowing me to use his X-rays that I used in this project.

I am also grateful to all my family members who believed in me during this extended thesis process.

ACADEMIC ETHICS AND INTEGRITY STATEMENT

I, Sait Emre Doğan, hereby certify that I am aware of the Academic Ethics and Integrity Policy issued by the Council of Higher Education (YÖK), and I fully acknowledge all the consequences due to its violation by plagiarism or any other way.

Name :

Signature:

Date:

ABSTRACT

A NOVEL HYBRID SCAFFOLD FOR MANAGING CRITICAL SIZE MANDIBULAR DEFECTS

This study provides a comprehensive approach to managing segmental mandibular defects. The patient's computed tomography images were used to design a patient-specific reconstruction plate. The mandible was reconstructed using virtual surgery, and new reference parameters were developed using craniometric and anatomical structures. Topology optimization and light-weighting were performed using the Voronoi and hollow patterns based on the areas with the most and least forces. The Voronoi pattern was used for the first time in topology optimization of a reconstruction plate. Structural analyses were conducted on the final designs. The Voronoi pattern is advantageous for clinical use, providing stability while using less material. The hollow design is effective, offering strength, screening for cancer recurrence, and easy removal after healing. A bioprinted bone scaffold was designed to improve function, healing, and aesthetics. An 0/90 hybrid scaffold (TCP-PCL enhanced with HA) was designed and manufactured using additive manufacturing methods. The printed scaffold was observed under a 40x microscope to assess the printing accuracy. Using a hybrid scaffold that mimics the original defect for a segmental defect is one of the novelties of this study.

Keywords: Bioprinting, Voronoi, Non-planar 3D Printing, Static Structural Analysis, FEA (Finite Elemental Analysis), Mandibular Reconstruction, Maxillofacial Segmental Defects

ÖZET

KRİTİK BOYUTTAKİ MANDİBÜLER DEFEKTLERİN YÖNETİMİ İÇİN YENİ BİR HİBRİT DOKU İSKELESİ

Bu çalışmada segmental mandibular defektlerin yönetilmesinde bütünsel bir yaklaşım geliştirmek amaçlanmaktadır. Segmental mandibular defektlerin rekonstrüksiyonu multidisipliner bilgi ve pratik gerektiren girift bir problemdir. Plak dizaynı için hastanın bilgisayarlı tomografi görüntüleri kullanıldı. Sanal cerrahiler ile defekt çıkarıldı ve mandibula rekonstrükte edildi. Mandibulanın sanal rekonstrüksiyonunda kranyometrik ve anatomik yapılardan yararlanılarak mevcut literatürde olmayan yeni referans parametreleri geliştirildi. Hastaya özel rekonstrüksiyon plağı tasarlandı. Çiğneme kuvvetlerine göre plak üzerinde en çok ve en az kuvvet binen alanların belirlenmesi için sonlu elemanlar analizi yürütüldü. Analiz sonuçlarına göre, voronoi ve boş paternlerden faydalanılarak topoloji optimizasyonu ve hafifletme yapıldı. Voronoi paterni mandibuler rekosntrüksiyon plağında topoloji optimizasyonu amacıyla ilk defa kullanıldı. Voronoi paterninin, plak imalatında hem yapısal stabilite sağlaması hem de malzeme kullanımını azaltması açısından faydalı olabileceği görüldü. Boşaltılmış dizaynın ise rekürrent kanserlerin izlenmesi, yeterli statik dayanım ve iyilişme sonrası çıkarılabilme şeklinde klinikte kullanılabilecek potansiyel özelliklere sahip olduğu görüldü. Tedavi sürecini geliştirmek amacıyla, biyobasım ile üretilmek üzere bir kemik doku iskelesi tasarlandı. 0/90 şeklindeki hibrit doku iskelesi (HA ile geliştirilmiş TCP-PCL) tasarlandı ve eklemeli imalat yöntemleri ile basıldı. Baskı doğruluğunu değerlendirmek için basılan doku iskelesi 40x mikroskop altında incelenlendi. Bu çalışmanın yenliklerinden birisi de segmental defekt için orijinal defektin şeklini taklit eden hibrit iskele kullanılmasıdır.

Anahtar Sözcükler: Biyobasım, Voronoi, Düzlemsel Olmayan üç boyutlu baskı, Sonlu Elemanlar Analizi), Mandibular Rekonstrüksiyon, Maksillofasiyal Segmental Defektler

TABLE OF CONTENTS

LIST OF FIGURES

LIST OF TABLES

LIST OF ABBREVIATIONS

FFF	Fibula Free-Flap
TCP	Tricalcium Phosphate
PCL	Polycaprolactone
HA	Hydroxyapatite
CT	Computed Tomography
STL	Standard Tessellation Language
FEA	Finite Elemental Analysis

1. INTRODUCTION

Trauma, cancer-related tissue, or organ losses have constituted severe health and economic issues throughout history and today. Due to its complexity, managing and reconstructing maxillofacial injuries and deformities need multidisciplinary knowledge and practice. [8–14]

The term tissue engineering appeared after the first successful kidney transplantation in 1954. [15] There are still two major options for managing organ or tissue loss: transplantation or implantation. The main challenges also did not change much: Limited donor supply, defect size, compromised healing, and complex anatomy. [1, 16] Organ transplantation is a viable option for some cases. Obviously, there are drawbacks, such as the need for a donor, immune response, and so on. Implantation is also a significant option for managing tissue defects. The idea of mimicking the native tissues in the scaffold implantation goes back to the 1990s. Langer and Vacanty laid the foundations of the contemporary scaffolds. Figure 1.1 Scaffold concepts have been improved significantly, from bioinert to biocompatible and lastly to bioactive implants, throughout the years. [17, 18] There were also improvements in designing and manufacturing complex scaffolds. Additive manufacturing techniques have emerged as the need for specific designs for each tissue engineering application. In the last decade, the bioprinting concept was proposed by Atala and Murphy. [19] A schematic illustration summarizes the process. [6] Figure 1.7 Lastly, Miranov and Ozbolat described bioprinting as follows:

"Computer-aided transfer process for simultaneous writing of living cells and biomaterials with a prescribed layer-by-layer stacking organization to fabricate bioengineered constructs for tissue engineering, regenerative medicine, or other biological studies" [20]

Restoring the mandible is challenging among the craniofacial tissues due to its

complex anatomy and physiology. The size and site of the defect is crucial. Also, if the surrounding tissue is included, the choice of treatment might alter majorly. Although no single classification system exists in the literature, an example is given to comprehend the issue. [2] Figure 1.2 for a clearer understanding of the subject. The mandible can move in three axes and six degrees of freedom, which makes masticatory movements unique. [3] Figure 1.3 The temporomandibular joint and masticatory muscles are responsible for these movements. Masticatory muscles differ in many ways, such as fiber type, diameter, and so on. Some muscles have intricate microstructures and tiny diameters, making them difficult to reconstruct. Therefore, after many reconstruction operations, physicians depend on physiotherapy to regain masticatory function. In addition, the literature on function loss and the life quality of patients after large reconstruction operations is strangely limited, and some of the existing studies rely on subjective information such as patient surveys. [14, 21–25]

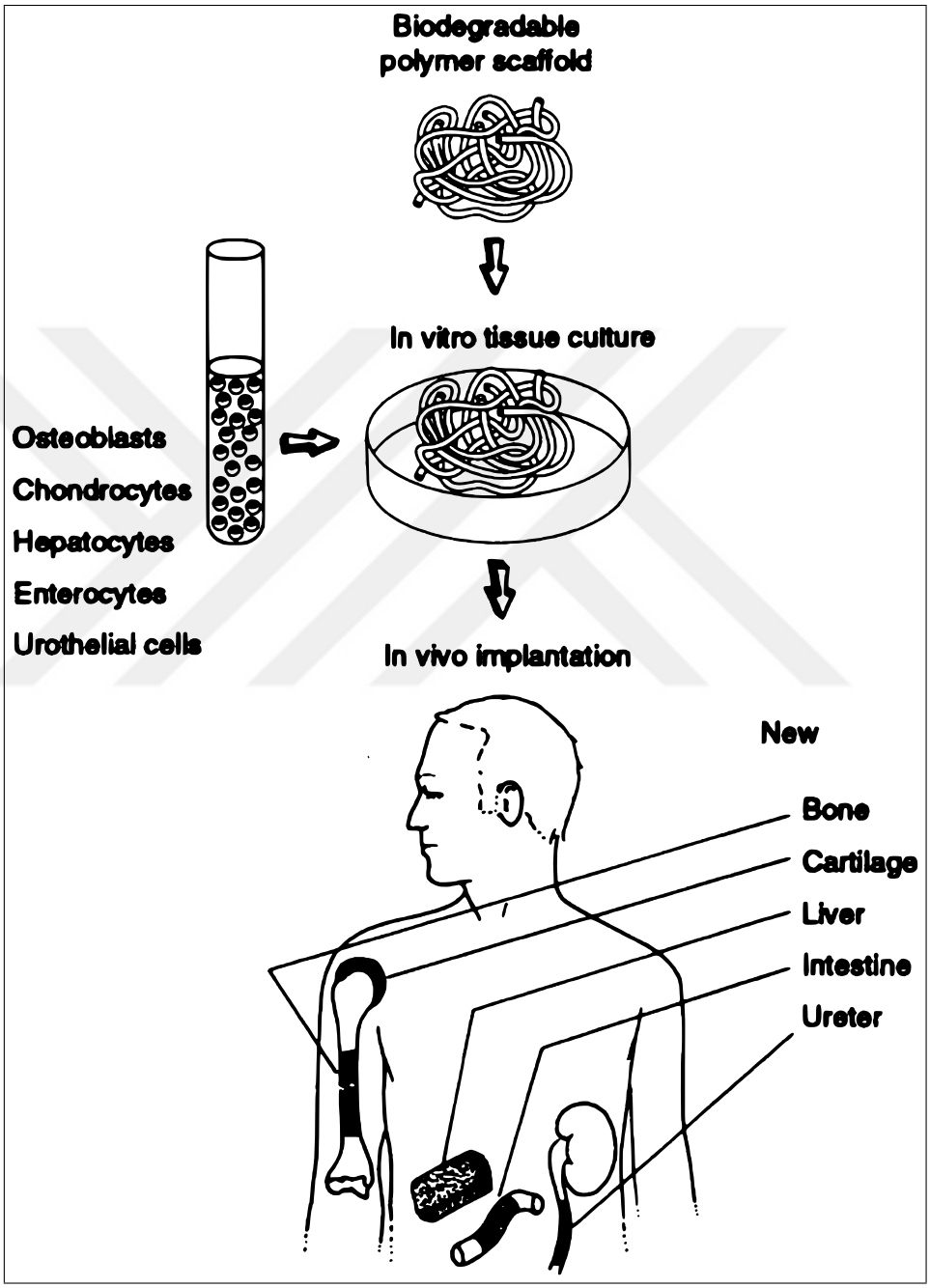

Figure 1.1 An illustration describing the first biomimetic scaffold definition [1].

		Bony defect		
		Anterior	Hemimandible	Lateral
		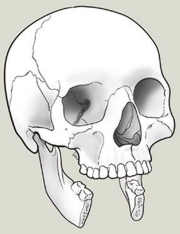	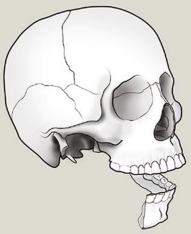	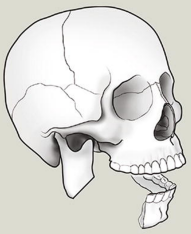
Soft tissue defect	None	IA	IIA	IIIA
	Intraoral only	IB	IIB1 ≤ 2 zones IIB2 ≥ 3 zones	IIIB
	Skin only	IC	IIC	IIIC
	Intraoral + skin	ID	IID	IIID

Figure 1.2 A table illustrating classification for segmental mandibular defects [2].

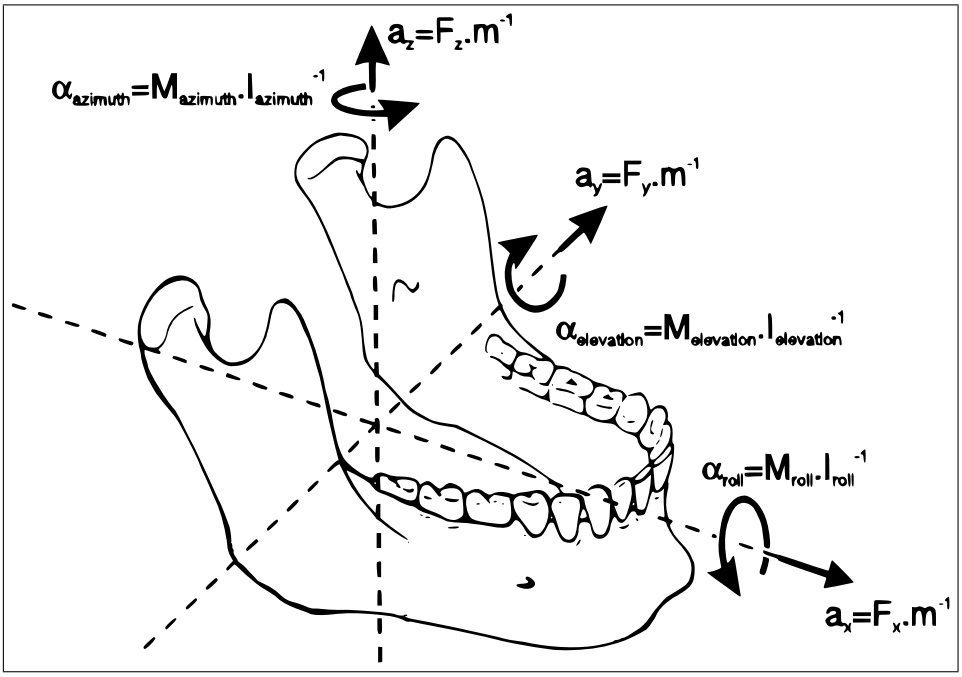

Figure 1.3 An illustration showing the 6 degrees of freedom for mandibular movement [3].

1.1 Management Strategies For Mandibular Segmental Defects

Currently, there are a few options for managing segmental mandibular defects:

Free-flap: Free-flap can be defined as transferring a patient's body part from its original site to the recipient site. A fibula free-flap is considered "the golden standard" in many literature cases. Depending on the defect site, defect size, and whether the soft tissue is included, the surgeon chooses a suitable donor site. Figure 1.4 An FFF has a high clinical success rate, and it can integrate the defect site without causing an immune response and can be adjusted depending on need. However, the drawbacks are still present, such as morbidity, requiring additional surgery, and so on. [2, 26–32]

	Fibula	Rectus Abdominis	Radial forearm (oc)	Scapula
				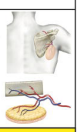
Bone	+++	-	+	++
Skin (surface area)	++	+++	++	++
Soft tissue (volume)	++	+++	+	++
Pedicle (length)	+++	+++	+++	+
Ease of harvest	++	+++	+++	+

(a)

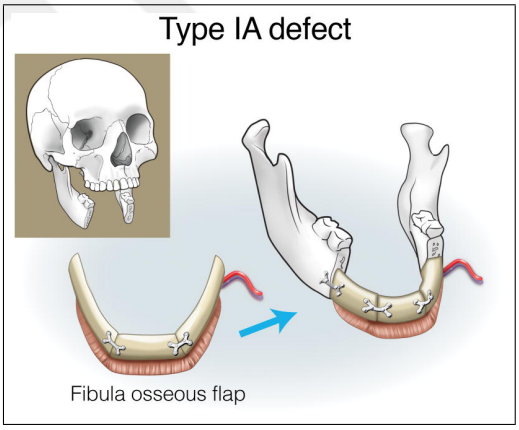

(b)

Figure 1.4 Different donor site options depending on the defect (a), an illustration reconstruction with a free flap (b) [2].

Induced Membrane/Masquelet Technique: The induced membrane technique, also known as the Masquelet Technique, consists of two stages. In the first stage, a spacer (often PMMA) is placed into the resection area to allow the development of a membrane around it and increase vascularisation for the second step. After the membrane is formed, the spacer is removed, and the desired bone graft is placed into the surgical area. Figure 1.5 Although it is mainly used in long bones, the induced membrane technique has been shown to be effective in reconstructing mandibular defects

in the literature. It is considered to be a relatively safe approach. However, there are potential complications such as failure of healing, infection, fracture of the bone graft, and so on. [4, 33–36]

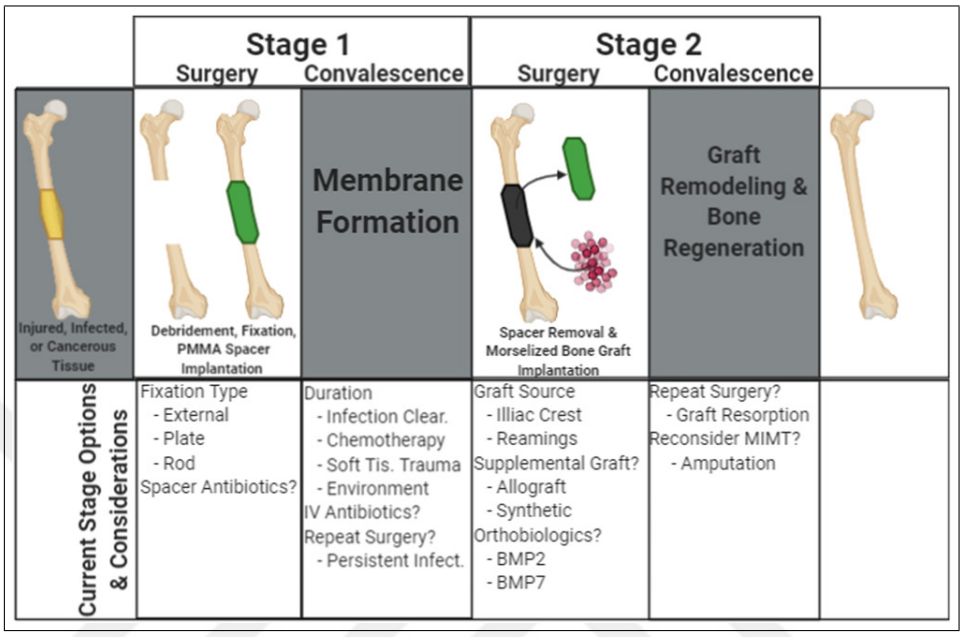

Figure 1.5 A schematic table illustrates the Induced Membrane Technique [4].

Distraction Osteogenesis: Distraction osteogenesis is a surgical procedure with multiple steps. Firstly, an osteotomy has been made to split the bone. Following that, a separator device is set up. The edges of the bone stay in contact for a while, and with the aid of the distractor device, they separate. This causes new bone formation through the gap. Figure 1.6 After the desired bone level is achieved, the device is removed. The advantages of this process can be summed up as follows. There is no need for a bone graft. Hence, any complications related to graft do not happen. For instance, there is no need for additional surgery to harvest the graft. It also provides soft tissue formation. Despite its potential, there are limitations and complications related to distraction osteogenesis. Failure of the fixations or device, malunion of the bones and relapse, infections, and possible nerve damage and psychosocial effects on patients. [5, 37–40]

Natural, Synthetic, and Hybrid Scaffolds: Using scaffolds might be an option for some cases. Additional surgery might not be available, and the defect might

be too small to use a free-flap. The physician might want to combine the scaffold with other techniques for a more patient-specific solution, and so on. [41–45]

Natural scaffolds are produced from biological sources derived from animals or plants. They offer a relatively higher biocompatibility and a better environment for cell attachment. The drawback is often the poor mechanical properties. Plus, managing the degradation rate might be challenging. [43, 45]

Synthetic scaffolds are often chosen for their superior mechanical properties to withstand the forces, tailorable physical and chemical properties suitable for various cases, and ease of manufacturing. The cell proliferation rates and biocompatibility are not their strong point, however. They are often made of polymers, ceramics, and so on. [46–50]

Hybrid scaffolds have emerged from the need and idea of concurrently having the advantages of synthetic and natural scaffolds. Since the native bone is composed of organic and inorganic components, the idea of fabricating hybrid scaffolds with organic and inorganic components has become widespread lately. Hydroxyapatite (Ca10(PO4)6(OH)2), a crystallized form of tricalcium phosphate, majorly forms the inorganic component of the bone. On the other hand, organic components of the bone are mostly composed of Type I collagen fibers. Different teams around the globe used various material choices based on this base idea. Table 1.1 illustrates different material compositions used in designing hybrid bone scaffolds in the literature. [43, 46, 51–72]

The choice of the material impacts the healing and cell proliferation. However, the material properties do not constitute the whole issue. The design of the scaffold is equally significant as the choice of material for this issue. Due to the limited budget, this study focused solely on the design process rather than both processes.

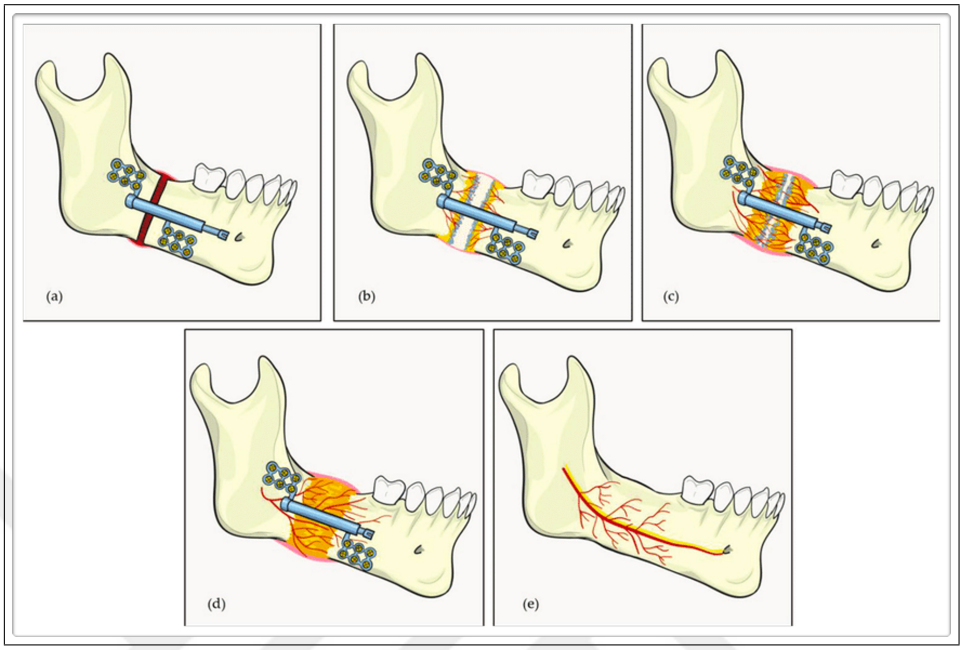

Figure 1.6 Illustration of the distraction osteogenesis process [5].

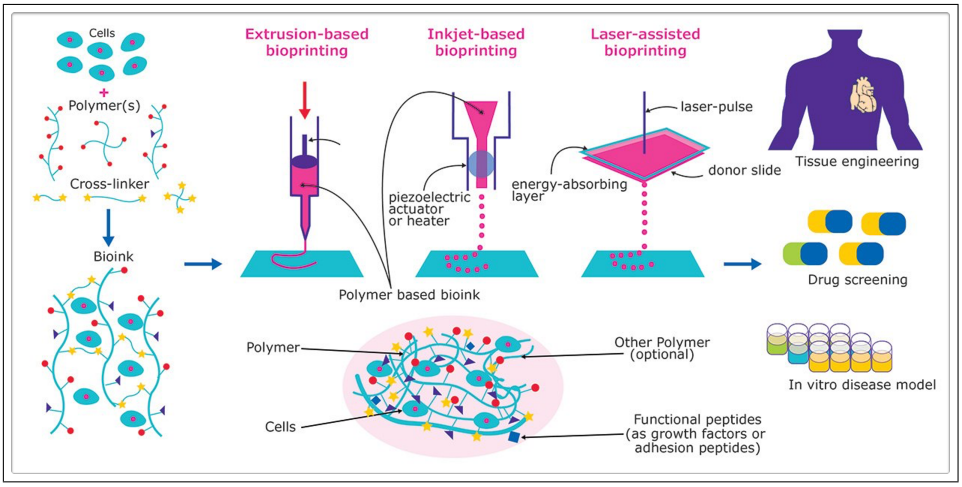

Figure 1.7 A schematic diagram depicts the bioprinting process [6].

Table 1.1 Different examples of mixing organic and inorganic components for preparing bone scaffolds.

	Inorganic Components	Organic Components	Preparation Methods	Year	Link
Amiryaghoubi et al.	poly (N-isopropylacrylamide), Graphen Oxide	Chitosan	Free-radical Copolymerization	2020	https://doi.org/10.1016%2Fj.ijbiomac.2020.06.138
El Fiqi et al.	Nanohydroxyapatite	Collagen	Sol-Gel	2020	https://doi.org/10.1016%2Fj.msec.2020.110660
Feng et al.	-tricalcium phosphate	PEEK, PLLA	Magnetic Stirring	2018	https://doi.org/10.1002%2Fadvs.201700817
Kim et al.	Hydroxyapatite	PCL	Polyurethane Foam Reticulation	2004	https://doi.org/10.1016%2Fj.biomaterials.2003.07.003
Kim et al.	Hydroxyapatite	PCL, Cellulose	Electrospinning, Modified Gas Foaming	2020	https://doi.org/10.1016%2Fj.carbpol.2020.116880
Lourenço et al.	Strontium-Hyroxyapatite	RGD Alginate	Crosslink	2019	https://doi.org/10.1016%2Fb978-0-12-820508-2.00009-x
Mohammadi et al.	Hydroxyapatite	Poly L-lactic acid	Electrospinning	2018	https://doi.org/10.1016%2Fj.nano.2018.06.001
Nandakumar et al.	Calcium Phosphate	Poly(ethylene oxide terephthalate)-poly(buthylene terephthalate)	Rapid Prototyping, Electrospinning	2013	https://doi.org/10.4161%2Fbiom.23705
Oliveira et al.	Hydroxyapatite	Chitosan	Freeze Drying	2006	https://doi.org/10.1016%2Fj.biomaterials.2006.07.034
Raucci et al.	Hydroxyapatite	Gelatine	Sol-Gel, Freeze Drying	2018	https://doi.org/10.1002%2Fjbm.a.36395
Shrestha et al.	Zinc Oxide	Polyurethane	Electrospinning	2017	https://doi.org/10.1016%2Fj.matdes.2017.07.049
Torgbo et al.	Hydroxyapatite, Magnetite	Bacterial Cellulose	Ultrasound Irradiation	2019	https://doi.org/10.1016%2Fj.matchemphys.2019.121868
Wei et al.	Tricalcium Phosphate	Silk Fibroin, Gelatin, Hyaluronic Acid	Crosslink	2019	https://doi.org/10.1016%2Fj.bioactmat.2019.09.001
Yang et al.	Hydroxyapatite	PLGA, Chitosan	Quaternization	2018	https://doi.org/10.1016%2Fj.actbio.2018.08.015

2. METHODOLOGY

2.1 Retrieving Radiographic Data and Segmentation

A CT scan of the head and neck region of a patient with diagnosed odontogenic myxoma was used for this project, with the patient's consent. Digital Imaging and Communications in Medicine (DICOM) files were imported to the ITK-SNAP 3.02, an open-source segmentation software, to segment the mandible. [73] "Active Contour" function was used for segmentation. According to the literature, suitable thresholding values were used for segmental and trabecular bone. [74] Figure 2.1 depicts the process. After segmenting the mandible, the segmentations imported to the Materialise Mimics 25.0 ® cortical and trabecular regions of the bone were separated with a boolean operation. The resulting segmentations were exported in STL format.

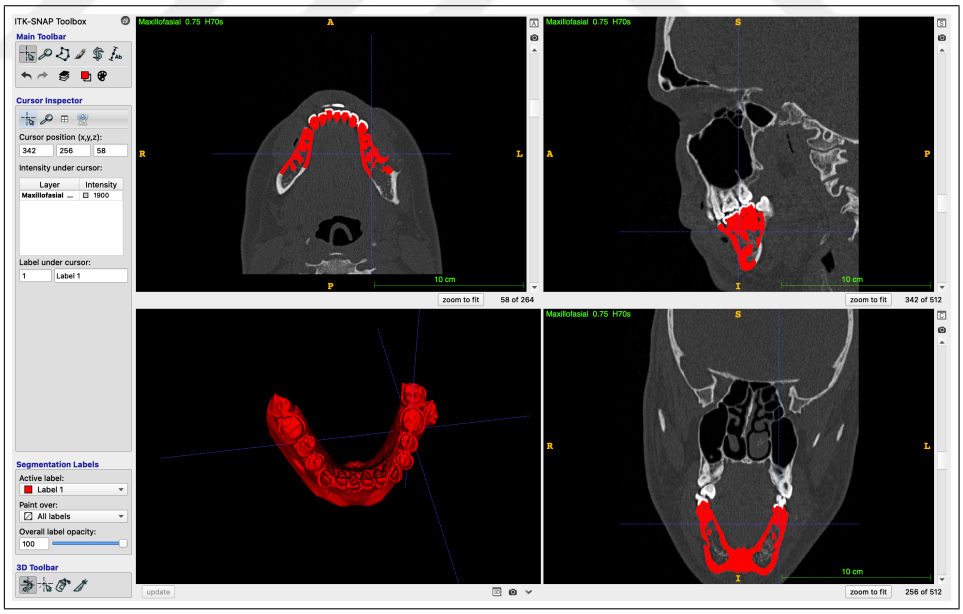

Figure 2.1 Segmentation process utilizing ITK-SNAP.

2.2 Model Design

For the plate design, Materialise 3-Matic 17.0 ® was used. STL files were imported. The defect area was removed (Figure2.2), and a mirroring operation was performed, taking into account anatomical landmarks such as Fovea Pyterigoidea, Condylion Laterale, Condylion Mediale, Spina Mentalis, and Protuberantia Mentalis to ensure the new model was in the correct position in the spacial plane. Novel referential entities were introduced to standardize the virtual reconstruction of the mandible. (Figure 2.3, 2.4, Table 2.1) Also, an outer line was followed through Margo Posterior Rami Mandibulae, Angulus Mandibulae, and Basis Mandibulae to ensure that the continuity of the bone was protected in the design. (Figure 2.4) The original and the new model depicted in Figure 2.5. Figure 2.6 shows the superimposed view of the two models. Since most of the scaffolds do not have the required force-bearing properties, the task of enduring the forces was assigned to the reconstruction plate. A base design for the reconstruction plate was created in the Materialise 3-Matic 17.0 ® selecting and offsetting the suitable area. While there is no consensus on the ideal thicknesses of the mandibular reconstruction plates in the literature, there are cases reported that surgeons use mostly 2-2.5 mm thick reconstruction plates for internal rigid fixation. [75] In this study, the thickness was adjusted to 2.5 mm. On the lingual side, the border of the reconstruction plate was positioned below the mylohyoid line, allowing the plate to carry the scaffold without obstructing the way of reconstructing muscles during operation. Aiming to reduce the stress shielding effect, the borders of the plate were elongated medially and distally. Screws with a diameter of 2.8 mm and a length of 7.5 and 10 mm were created for fixation. Figure 2.7 outlines the design process. Figure 2.8 shows the base model used for topology optimization and lightweight, plus the first model for FEA Analysis.

Table 2.1 The definition of referential entities.

Referential Entities	Definition
L_{CM-CM}	The distance between right and left condylion mediale
L_{FP-FP}	The distance between right and left fovea pterygoidea
L_{CL-CL}	The distance between right and left condylion laterale
L_{PM-FP}	The distance between protuberentia mentalis and fovea pterygoidea
L_{SMS-CM}	The distance between spina mentalis superior and condylion mediale
L_{SMI-CL}	The distance between spina mentalis inferiore and condylion laterale
$CL_{SMS-SMI}$	Connecting line between spina mentalis superiore and spina mentalis inferiore

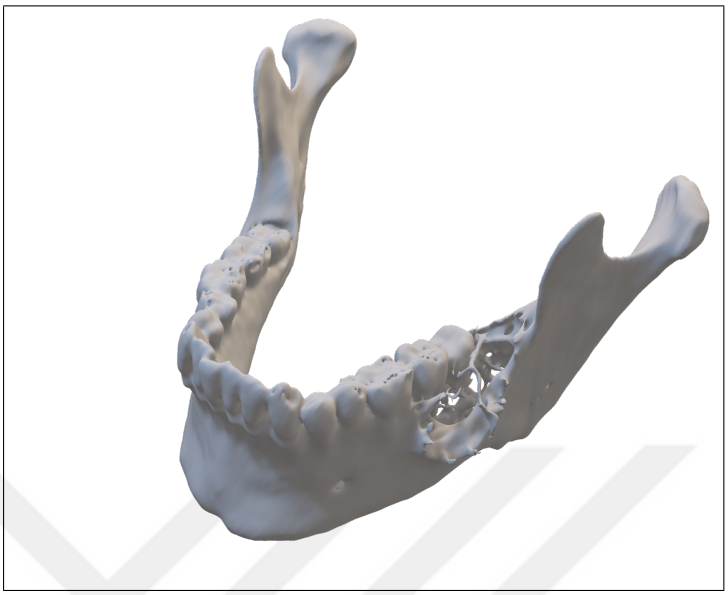

(a)

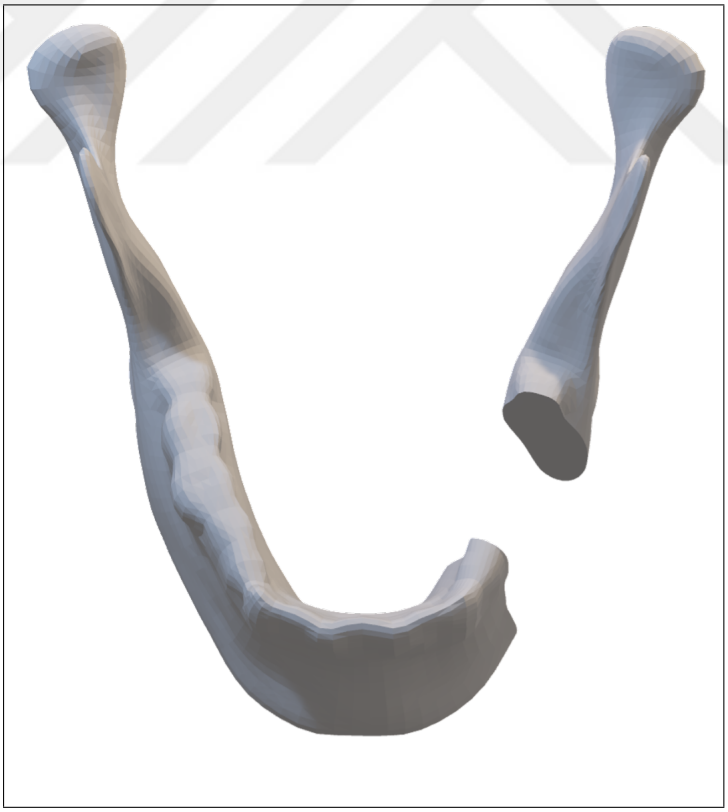

(b)

Figure 2.2 Segmentation of the mandible(a), after virtual surgical resection, the defect area has been removed (b).

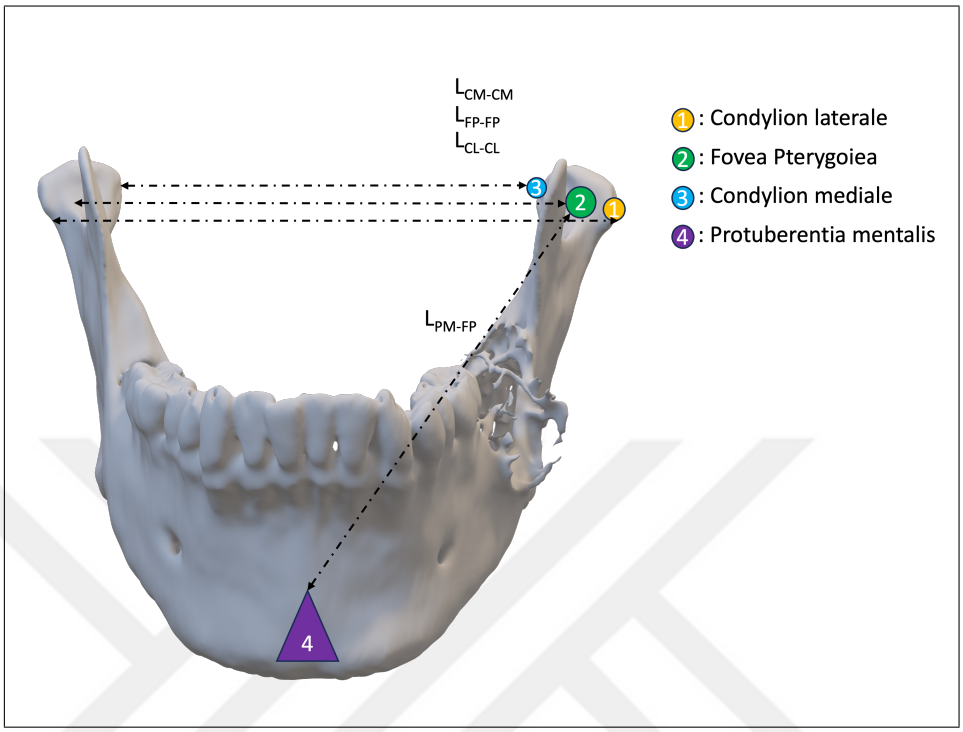

(a)

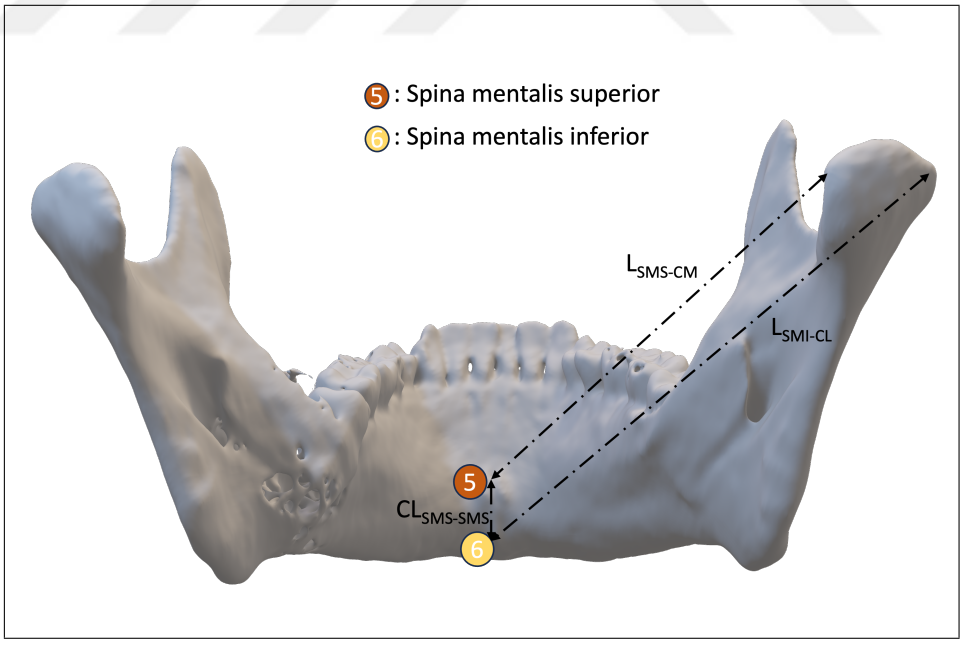

(b)

Figure 2.3 Anatomical landmarks and referential entities on the original model used in the mirroring process. Conylion regions, fovea pterygoidea, protuberentia mentalis (a); Spina mentalis regions, and conylion regions(b).

(a) (b)

Figure 2.4 Some of the anatomical landmarks that have been used in mirroring (a), the line followed through Margo Posterior Rami Mandibulae, Angulus Mandibulae, Basis Mandibulae (b).

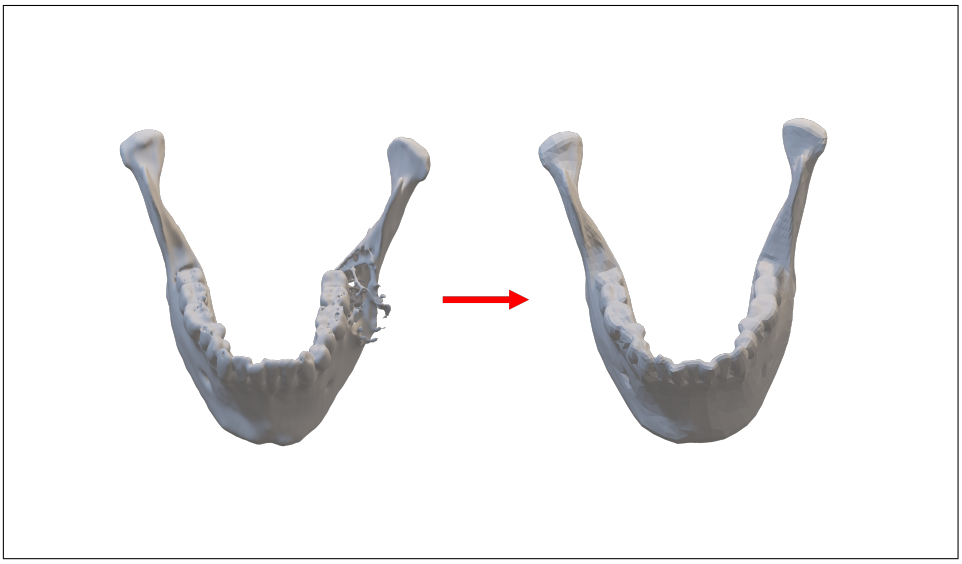

Figure 2.5 The transition of the model from original to mirrored.

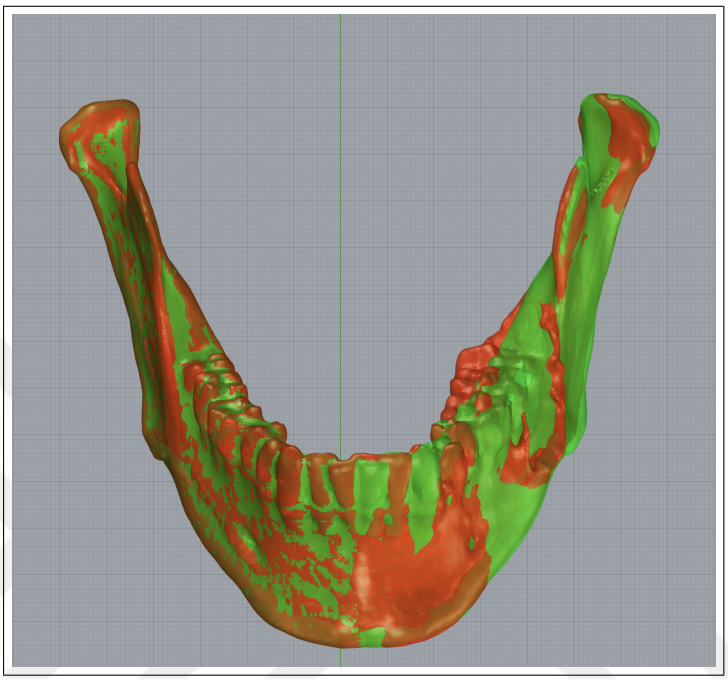

(a)

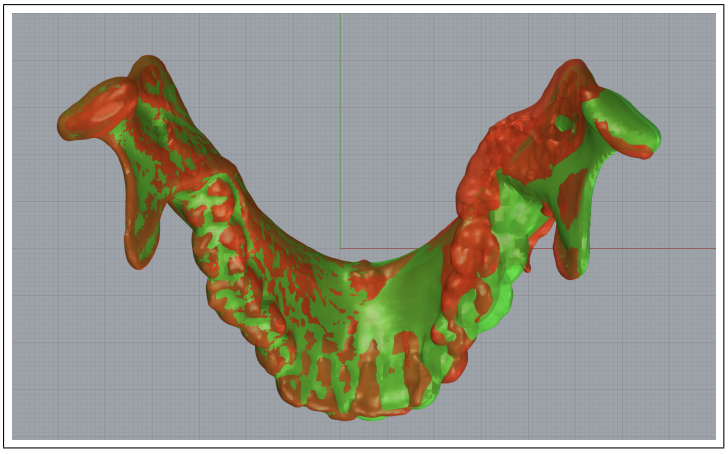

(b)

Figure 2.6 The superimposed view of the original and mirrored mandible model. Note how the dental arc shifted due to the expansion of the neoplasm.

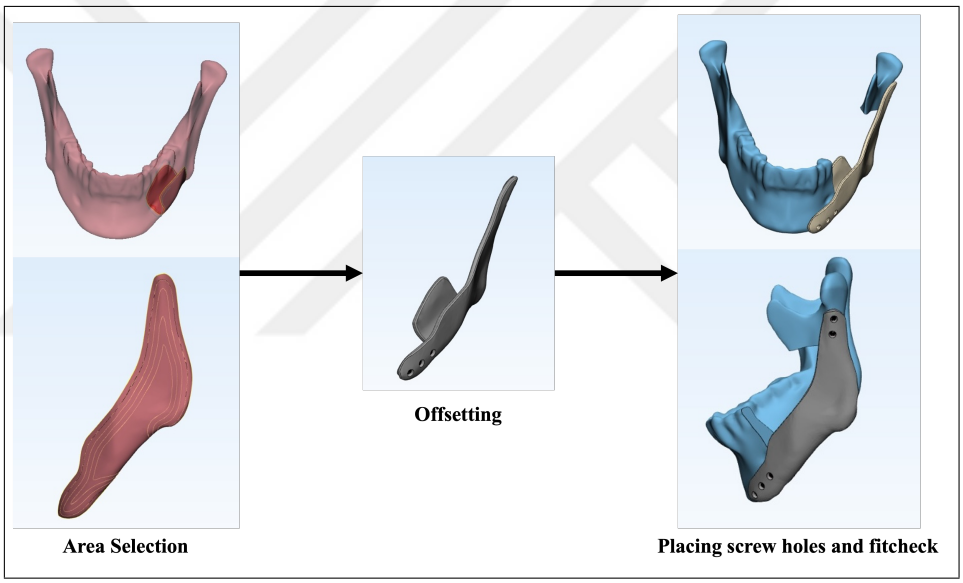

Figure 2.7 Design process.

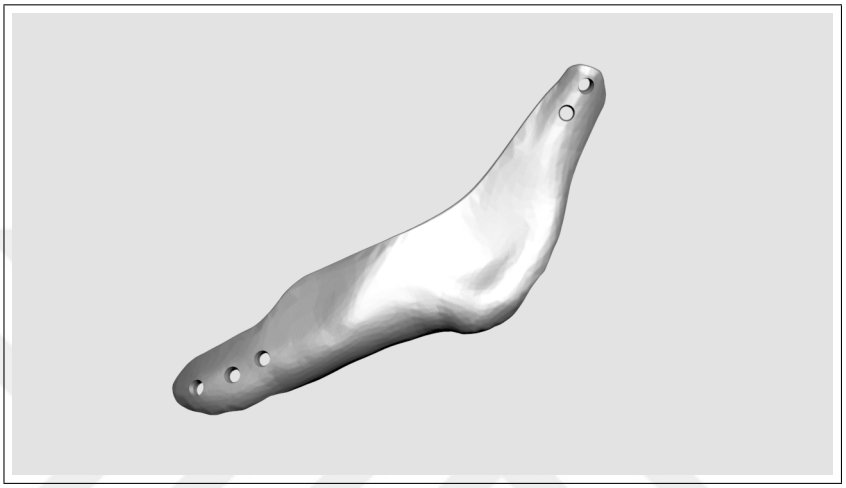

(a)

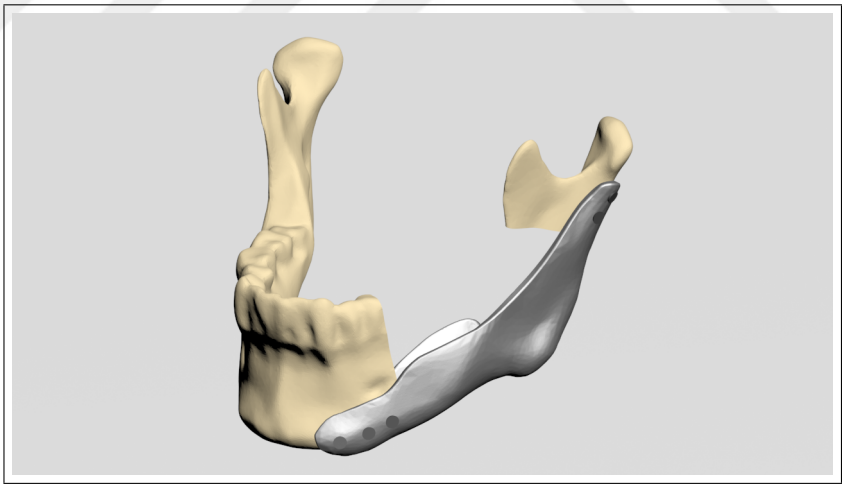

(b)

Figure 2.8 The first plate design for topology optimization and lightweighting(a), the first model for FEA Analysis (b).

2.3 FEA Analysis and Topology Optimization

Designed models were imported to the ANSYS (ANSYS Inc., USA) for static structural analysis.

Among the other titanium alloys, Ti-6Al-4V stands out for various reasons: It is easier to manufacture complex structures, as in this study. It has favorable material properties such as low density, biocompatibility, high corrosion resistance, and so on. Combining it with additive manufacturing techniques, superior surface finishings can be achieved. Plus, it is cheaper than similar titanium alloys with better biocompatibility properties, including Ti–6Al–7Nb, and Ti–5Al–2.5Fe. In the literature, Ti–6Al–7Nb was considered superior. Zhang et al. considered Ti–6Al–7Nb has better biocompatibility properties for craniofacial defects depending on a conference paper. Ti–6Al–7Nb was used for cranial implants in rats. Although no inflammatory reactions were reported, there was also no osseointegration or newly formed bone structure in the mentioned study. [76–78] Consequently, because of the favorable characteristics mentioned above, Ti-6Al-4V is the most commonly used biomedical alloy and is frequently used in reconstruction surgeries. [77, 79] The material choice for the reconstruction plate was Ti-6Al-4V in this study.

Material properties given in Table 2.2 were provided from the relevant literature. [80–83]

Masticatory muscle forces were limited to two major tasks: constrained left molars and constrained right molars. Table 2.3 shows the muscle force values. Considering the previous literature, these tasks showed the greatest force in similar segmental mandibular defects. Figure 2.9 illustrates the muscle forces and boundary conditions. [7, 80, 81, 84] The results of the first analysis are given in Figure 2.10 and Appendix.

Table 2.2 Material properties used in the FEA Analysis.

	Elastic Modulus (GPa)	Poisson's Ratio	Yield strength (MPa)	Young's Modulus
Ti-6Al-4V	115	0.323	107	115
Cortical Bone	12	0.3	88	96.2
Trabecular Bone	1-2	0.3	3.9	96.2
Titanium Screws	110	0.3	850	116

Table 2.3 The muscle forces performing clenching tasks. Raw data was acquired from the literature. [7] Muscular forces: SM-superficial masseter, DM-deep masseter, MP-medial pterygoid, ILP-inferior lateral pterygoid, AT-anterior temporalis, MT-middle temporalis, PT-posterior temporalis.

Clenching Tasks	**Side**	**Direction**	**Muscular Force**							**Constraint**
			SM	***DM***	***MP***	***AT***	***MT***	***PT***	***ILP***	
Right Unilateral Molar Clench	Right	Force	137.1	58.8	146.9	115.4	63.1	44.6	20.1	**Constrained right molars**
		Fx	-28.4	-32.1	71.4	-17.2	-14.0	-9.3	12.6	
		Fy	121.2	44.5	116.1	114.0	52.8	21.1	-3.5	
		Fz	57.4	-21.0	54.8	5.1	-31.5	-38.1	15.2	
	Left	Force	114.2	49.0	104.9	91.7	64.0	29.5	43.5	
		Fx	23.6	26.7	51.0	13.7	14.2	6.1	27.4	
		Fy	101.0	37.1	83.0	90.5	53.6	14.0	7.6	
		Fz	47.9	17.5	39.1	4.0	32.0	25.2	32.9	
Left Unilateral Molar Clench	Right	Force	114.2	49.0	104.9	91.7	64.0	29.5	43.5	**Constrained left molars**
		Fx	23.6	26.7	51.0	13.7	14.2	6.1	27.4	
		Fy	101.0	37.1	83.0	90.5	53.6	14.0	7.6	
		Fz	47.9	17.5	39.1	4.0	32.0	25.2	32.9	
	Left	Force	137.1	58.8	146.9	115.4	63.1	44.6	20.1	
		Fx	28.4	32.1	71.4	17.2	14.0	9.3	12.6	
		Fy	121.2	44.5	116.1	114.0	52.8	21.1	3.5	
		Fz	57.4	21.0	54.8	5.1	31.5	38.1	15.2	

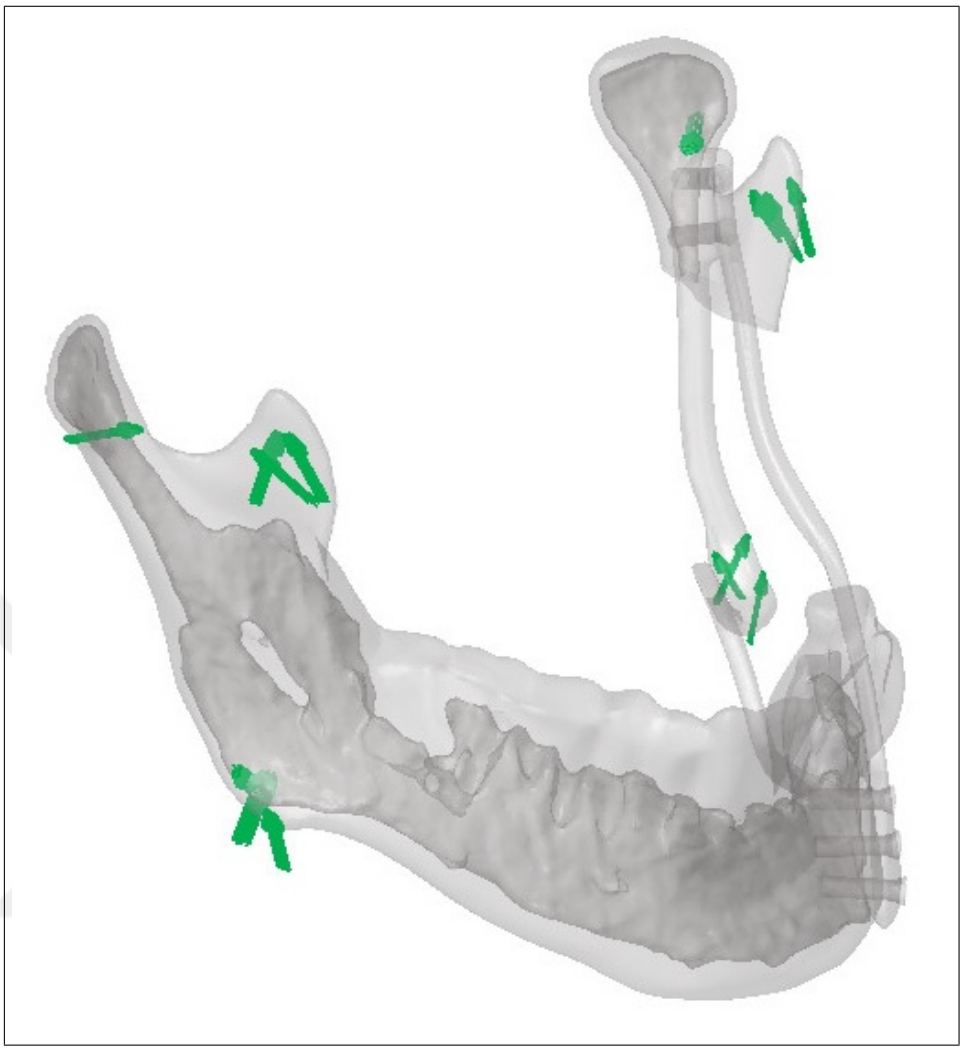

Figure 2.9 Boundary conditions, segmented trabecular, and cortical bone are shown on the hollowed model.

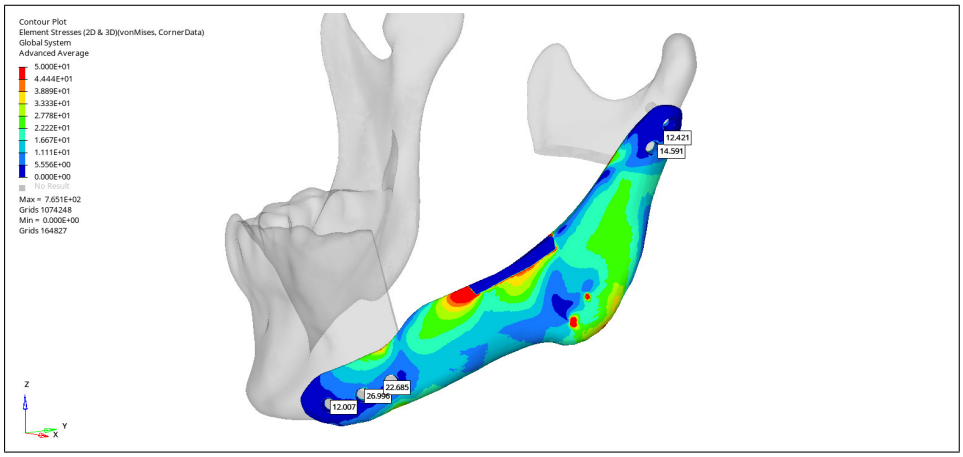

(a)

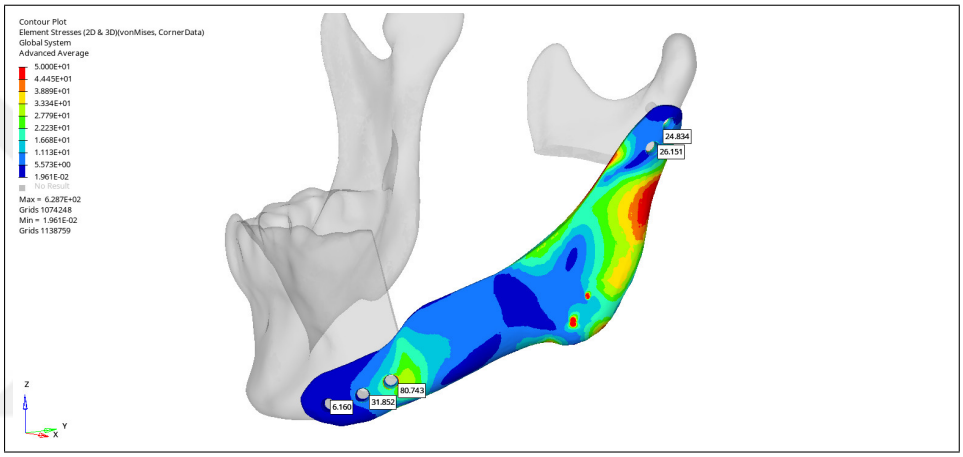

(b)

Figure 2.10 The forces when clenching left molars (a), and right molars (b).

2.4 Topology Optimization

According to the first analysis results, the areas with the most stress were detected. Two new designs were developed for different purposes. The first strategy was hollowing the reconstruction plate for visibility of the defect area for screening a cancer-recurrence scenario after the surgery without losing the ability to carry the scaffold. The latter used a specific pattern named "Voronoi" for effectively lightweight without losing the load-bearing properties. Voronoi tesselation was used for cranial implants before in the literature because of its customizable character and anisotropic properties. The cranial plate was customized specifically for the patient, considering the forces. [85–87] A similar approach was followed in this study. Figure 2.11 shows the second custom designs. In the topology optimization process in the plate with

Voronoi pattern, the areas with the most stress were fed with extra points (attractor points) to increase the material in the region. The areas with the least stress were fed with fewer points to reduce the material. The points were used to create a 3D Voronoi tesselation. For the hollowed design, new borders created a line with a 2.5mm diameter following the outer layer and the stress areas, leaving the middle part open for screening purposes.

The results of the second analysis showed that both designs are capable of withstanding the muscular forces when chewing.

Under the task of clenching with left molars, in the hollow design, the most extreme stress was located on the lingual site. Plus, the titanium screw at the condylar region(the one far away from the defect) had the most stress. When clenching with the right molars, the most extreme stress was located closely on the base region of the mandible. The maximum stress was under the limits of the material; hence, it can be expected to have potential in real clinical cases.

The plate with Voronoi tesselation showed a more even stress distribution. Maximum stress values were far below the material limits at both clenching tasks. Titanium screws showed similar results comparing the screws with the hollowed plate. It can be anticipated that the plate with the Voronoi pattern can endure clinical scenarios. The results of the second analysis are provided in Figure 2.12, Figure 2.13, and in detail in the Appendix.

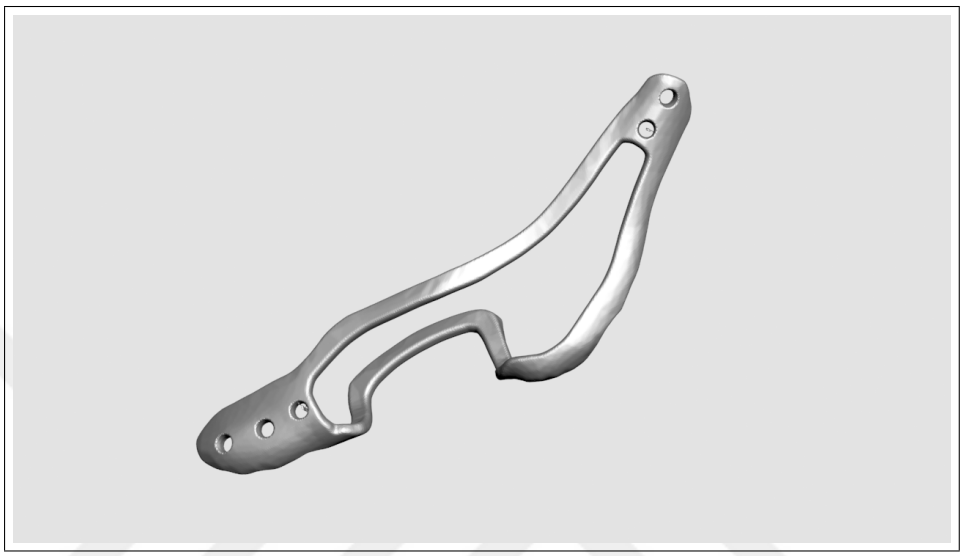

(a)

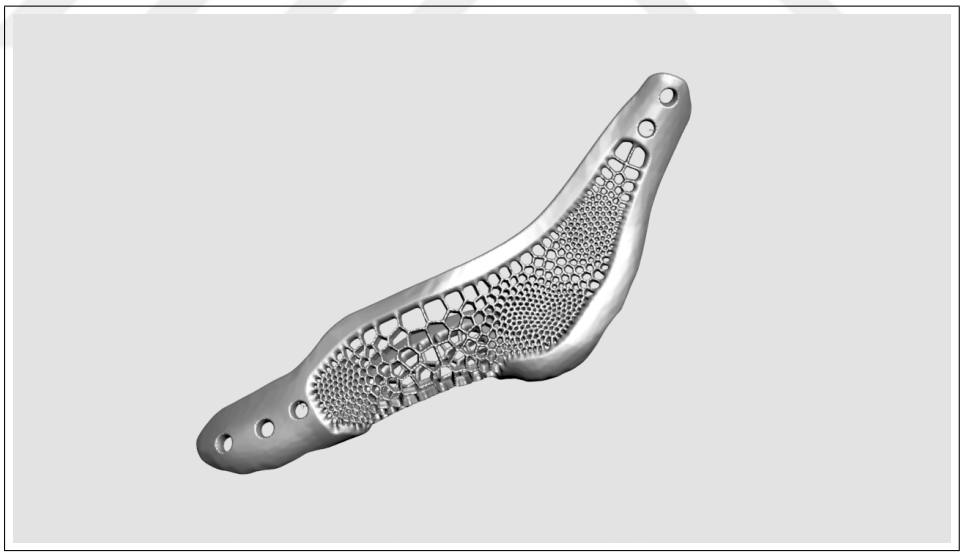

(b)

Figure 2.11 The hollow plate (a), and Voronoi plate (b).

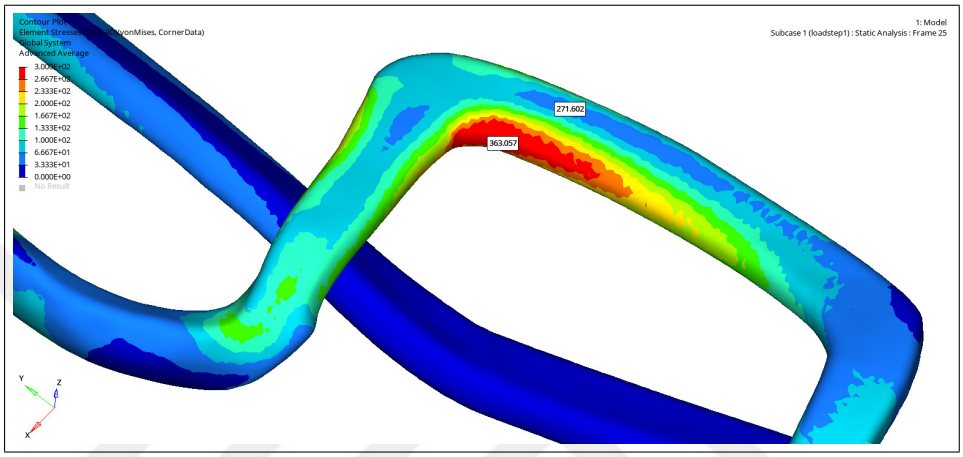

(a)

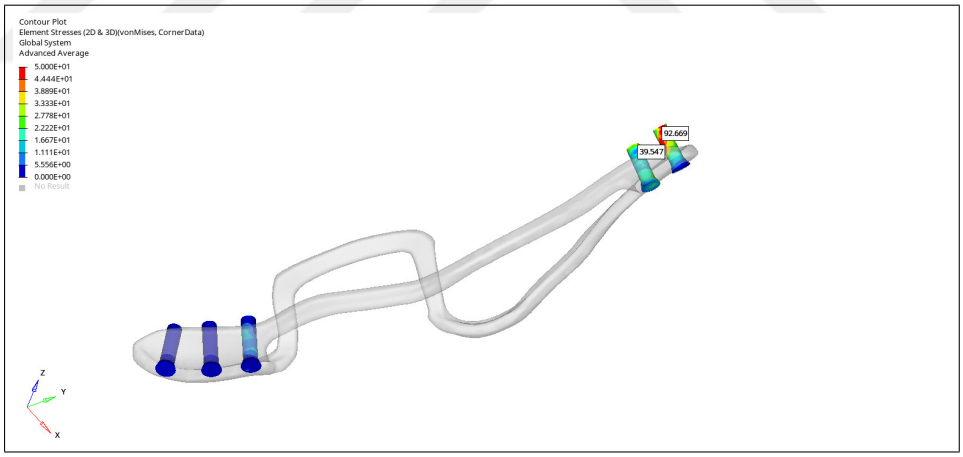

(b)

Figure 2.12 Stress distribution of hollowed design with clenching with left molars (a), and titanium screws(b).

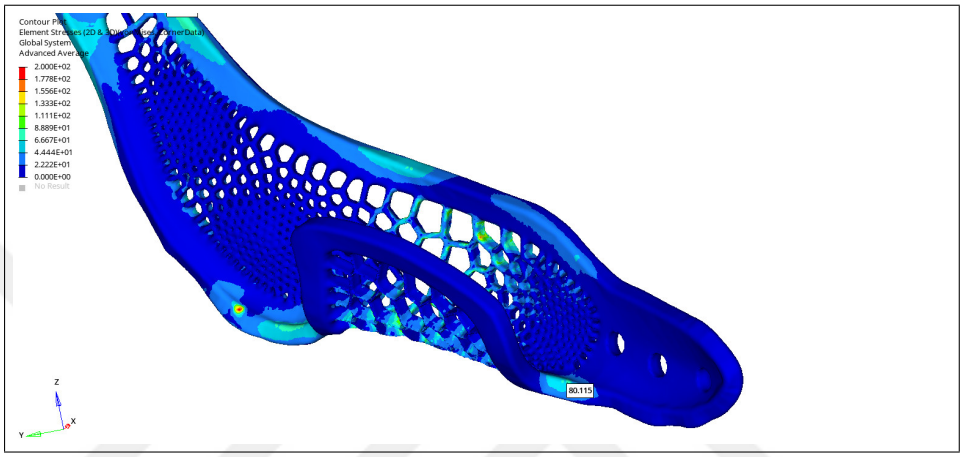

(a)

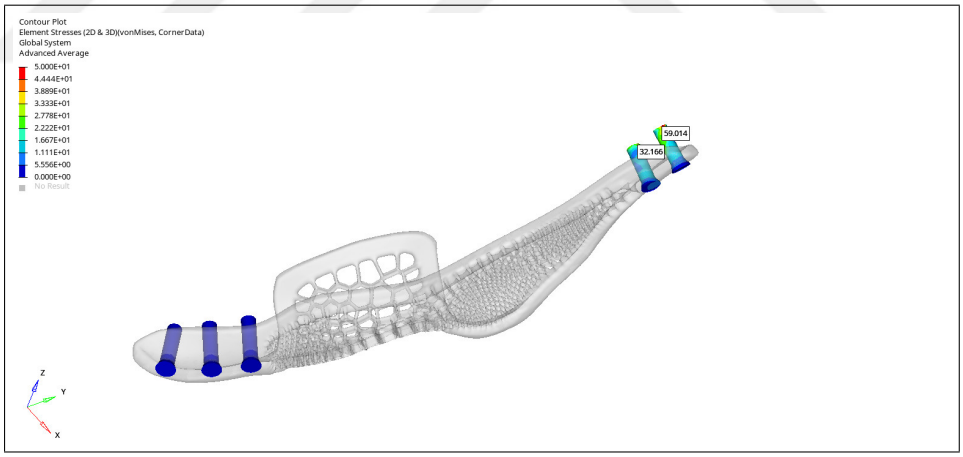

(b)

Figure 2.13 Stress distribution of the Voronoi design with clenching with left molars (a), and titanium screws(b).

2.5 Toolpath Planning and Designing Scaffold

The objective of the current study was to create a porous hybrid scaffold that could be utilized to repair a defect site. To achieve this, the team employed slicing software (Ultimaker CURA 4.6.1) and used Figure 2.14 to illustrate the design. The scaffold was manufactured using a commercially available blend of Tricalcium phosphate (TCP) and Polycaprolactone (PCL), which were then strengthened with a Hydroxyapatite (HA) dip coating (Bioscaffold Bloocell®). Tricalcium phosphate was chosen as the inorganic matrix due to its osteoconductive properties, while Polycaprolactone has been established as an approved material for various biomedical applications. Using the combination of PCL-TCP on scaffolds has been shown to be more efficient than using them individually. These scaffolds demonstrated excellent biocompatibility, with favorable cell proliferation and adhesion rates. Furthermore, their biodegradability makes them an ideal candidate for controlled drug delivery applications, as demonstrated in prior literature. This material combination is clinically significant as it can potentially be loaded with anti-cancer drugs onto these scaffolds to prevent recurrent cancers. To fabricate the scaffold, a commercially available 3D bioprinter, Bloocell®, was used, and Figure 2.15 illustrates the printed scaffold. The nozzle diameter was tuned to 2mm while adjusting the pore size to 400 µm to achieve a pore size that is satisfactory for vascularization and mineral deposition while ensuring that the mechanical properties of the scaffold were not compromised. After printing, the scaffolds were inspected under the microscope. The image displayed in Figure 2.16 provides a close-up view of the scaffold under a x40 zoom. Figure 2.17 shows the integrated image of the defect, Voronoi Plate, and the scaffold to visualize the planned results.

For future studies, a novel scaffold design was also introduced. The scaffold design was based on mimicking the mirrored version of the defect area. Rhinoceros 3D, Version 7, and Grasshopper were used to design the scaffold and create a toolpath planning using PythonScript. A pattern for bone scaffolds in the literature was used to mimic the fibula. [88] The optimum pore size for bone is specified in the range of 200-900 µm, although there is no consensus. Pores were designed to expand from 250 µm to 900 µm from the inside of the scaffold to the outside. Figure 2.18 shows a part of

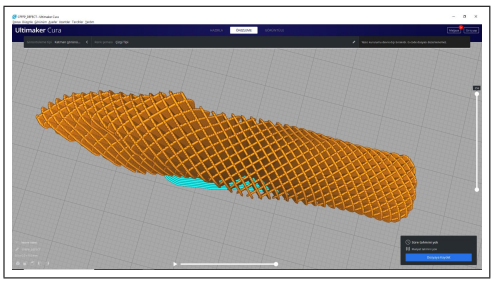

(a)

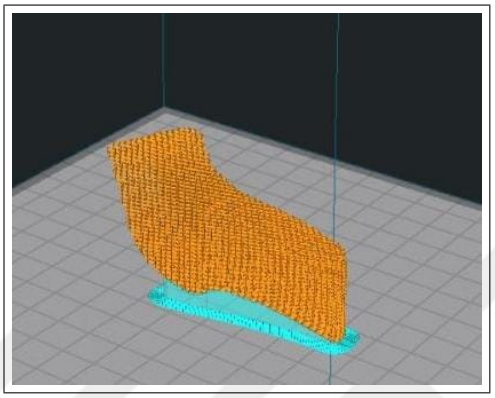

(b)

Figure 2.14 Design process of the scaffold.

the scaffold design for comprehension of the pattern. A gap is also created inside the graft for various potential uses: Placement of the inferior alveolar nerve during surgery. Creating a potential reservoir for drugs. Creating a reservoir for the autologous bone graft to ensure the continuity of the bone might be beneficial for the healing process. Figure 2.19a Printing the scaffold while protecting the pattern is another challenge due to the curvature of the angle of the mandible. Non-planar printing techniques might be beneficial for this issue. Changing the printing diameter during printing might be a viable strategy. Figure 2.19b illustrates a side view of the scaffold and the tilting axes to comprehend the basic idea of non-planar printing.

(a) (b)

Figure 2.15 Printed scaffold with a support structure (a), after removing the support structure(b).

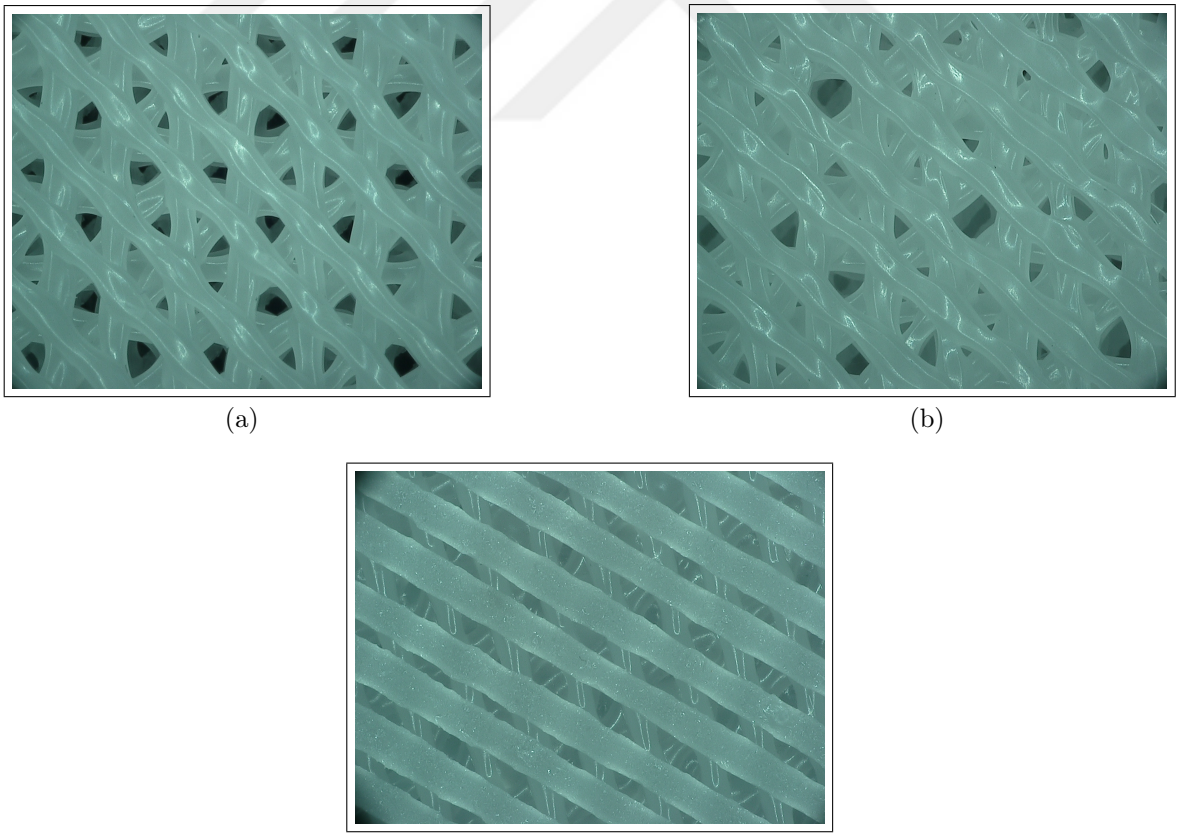

(a) (b)

(c)

Figure 2.16 The scaffold structure under the 40x zoom microscope.

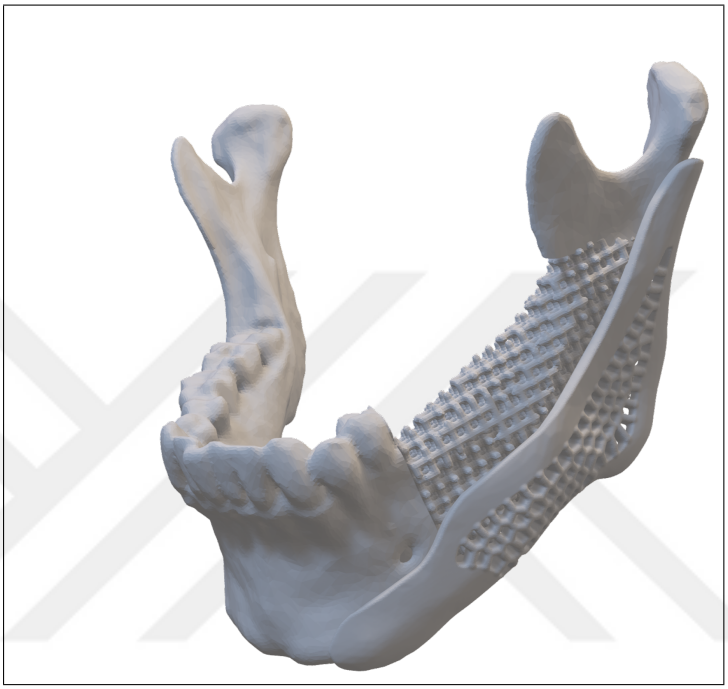

(a)

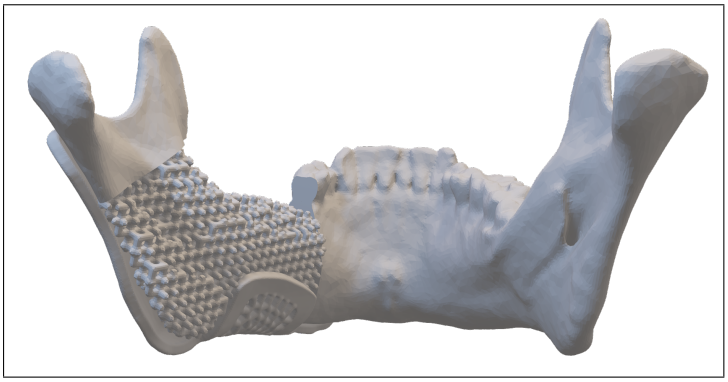

(b)

Figure 2.17 The integrated image of the defect, Voronoi Plate, and the scaffold. The plate and the scaffold mimic the native tissue.

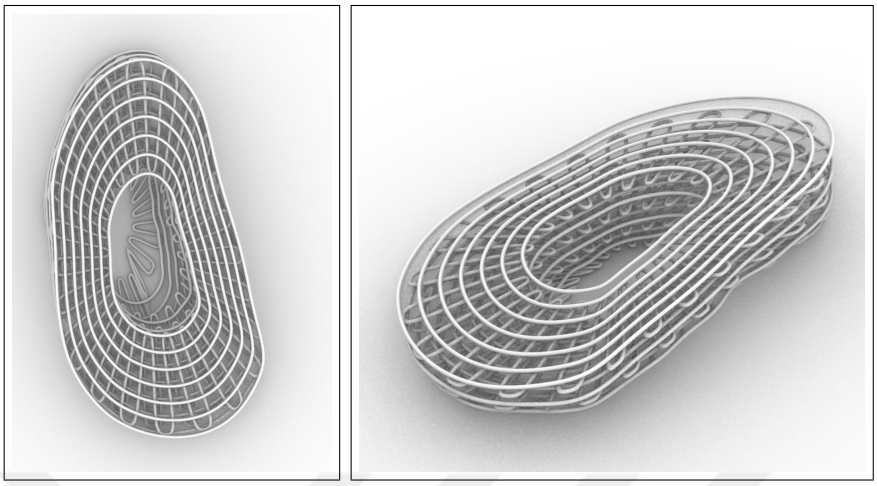

(a) (b)

Figure 2.18 A part of the scaffold and the printing pattern is visualized (a,b).

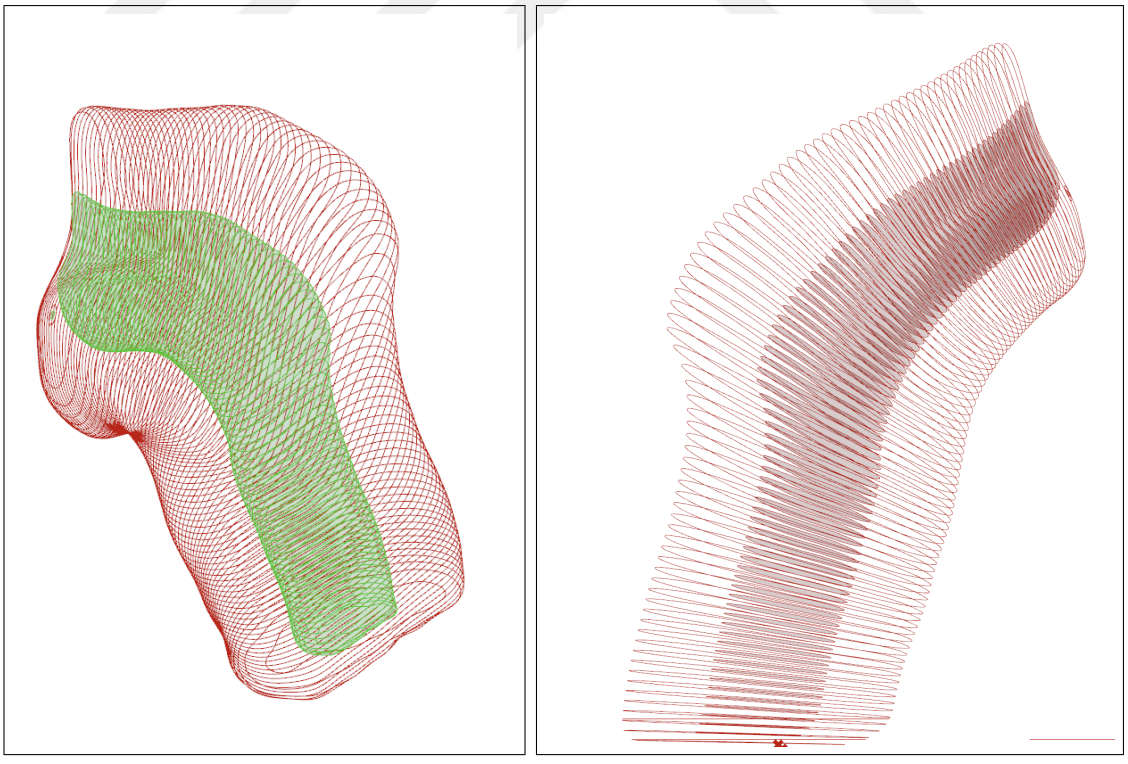

(a) (b)

Figure 2.19 The created gap inside the scaffold (a), side view of the scaffold with tilting axes(b).

3. RESULTS AND DISCUSSION

This thesis presents a novel hybrid scaffold system for managing segmental mandibular defects by integrating the reconstruction plate and scaffold. The study focuses on developing patient-specific reconstruction plates through finite elemental analyses to improve the reconstruction process. In order to enhance the standardization of the virtual reconstruction process, a set of novel parameters has been developed utilizing craniometrics and anatomical landmarks. The first plate was designed with properties that surpass the masticatory forces. To cater to different requirements, a hollow design was tailored for screening purposes, while a design based on Voronoi tessellation was tailored for load-bearing purposes, considering the finite element analysis (FEA) results. This study employs the Voronoi tessellation for the topology optimization of mandibular reconstruction plates for the first time. The mass of the human mandible lacks a standard value, and previous studies report it to be in the range of 90.85g $\pm$ 16.08 for wet mandible mass. [89] Based on this range, the mass of the defect was calculated to be 20.3g $\pm$ 3.6. Optimization and lightweight techniques were implemented, resulting in the Voronoi and hollowed designs providing a mass loss of % 37 and % 55.34, respectively, approaching the weight of the original mandible. (Table 3.1 and Figure 3.1) Using Voronoi tessellation might be a promising tool for designing mandibular reconstruction plates with anisotropic properties. Figure 3.2 illustrates the graphical abstract of the processes.

For future studies, advanced study models that accurately reflect the complex three-dimensional masticatory configuration of the mandible and account for biological factors are required. [90–93] Further mechanical testing of the plates is also essential, given the limitations of current testing systems. Developing more sophisticated testing methods that provide accurate and reliable results is crucial.

The study utilized a TCP-PCL hybrid scaffold augmented with HA dipping to enhance the healing process by using organic and inorganic components, a promising

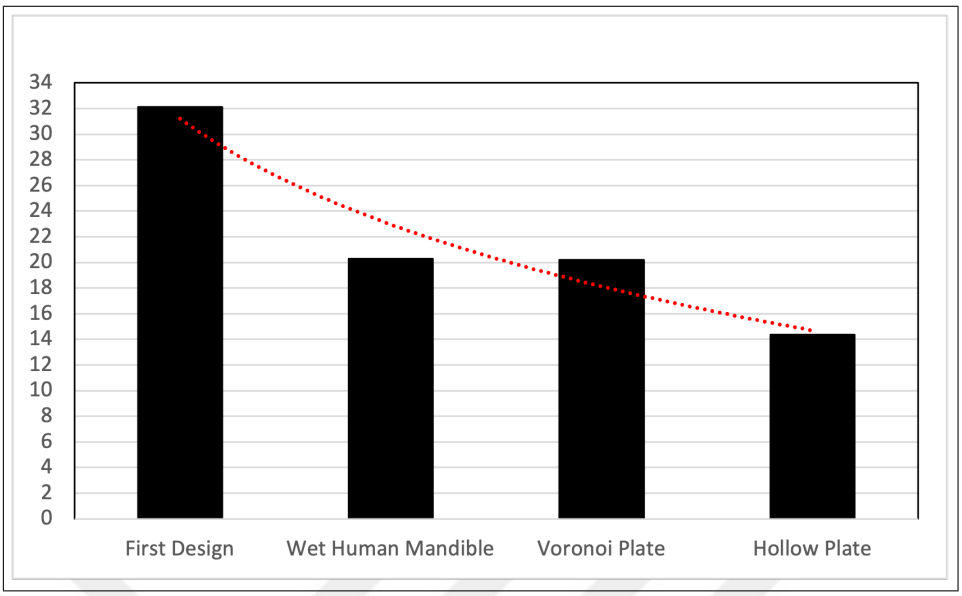

Figure 3.1 The chart illustrates the weights of the wet human mandible and designed reconstruction plates.

	Weight (grams)	Lightweighting (%)
First Designed Plate	32,1893556	x
Wet Human Mandible	20,3	x
Voronoi Plate	20,210304	37,2143254
Hollow Plate	14,3742504	55,3447091

Table 3.1 The results of the lightweighting process.

approach for promoting tissue regeneration and improving patient outcomes. However, bone regeneration remains a significant challenge, requiring different material selection, characterization, and in-vitro studies of scaffolds. Currently, none of the developed graft or scaffold systems has been able to replicate native bone tissue fully. Numerous areas require improvement, including the formation of complex-structured scaffolds, the duration of cell viability and efficacy of cell seeding, poor mechanical properties, biocompatibility issues, design challenges, and pore sizes and shapes. [90, 94–97]

A novel scaffold design was introduced based on mimicking the mirrored version of the defect area, using a pattern for bone scaffolds in the literature to mimic the fibula. Printing the scaffold while protecting the pattern is challenging due to the curvature of the angle of the mandible. Non-planar printing techniques may be beneficial for this issue.

Before the clinical implementation of our plate designs and scaffold-plate system,

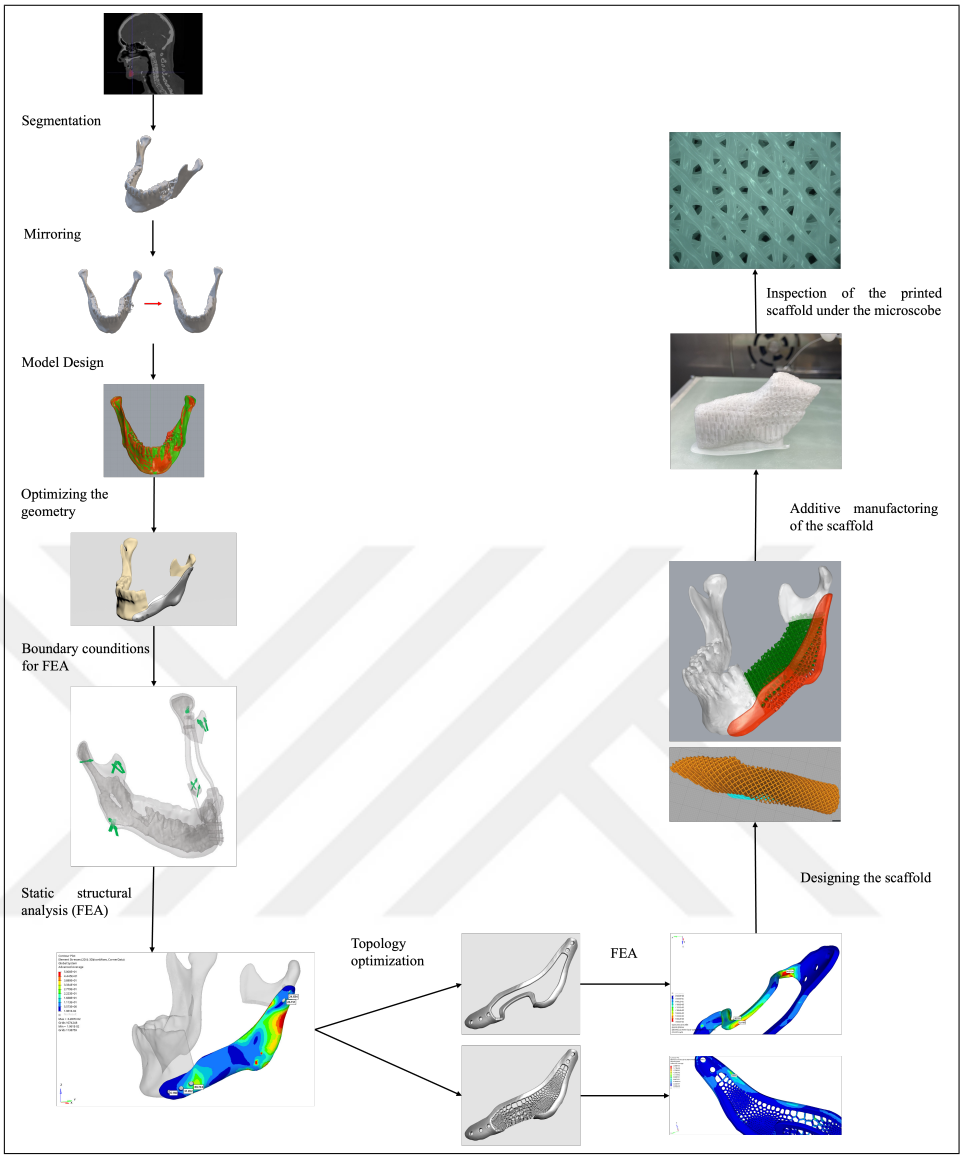

Figure 3.2 Graphical abstraction of the processes.

animal studies after in-vitro testing are imperative to evaluate the overall efficacy of the components. Modulating the pore size between 200-900 µm could imbue the scaffold with increased biomimetic properties. Within this range, larger pore sizes have been observed to exhibit a positive correlation with increased calcification and vascularization, thereby targeting the cortical bone region. In comparison, smaller pore sizes are more suitable for the trabecular bone region. [98, 99]

It is worth noting that despite significant progress in the field of tissue engineering, free tissue flaps continue to be regarded as the gold standard for managing large

segmental defects. Bioprinting bioactive scaffolds has emerged as a promising strategy for addressing this issue. However, managing critical-size bone defects is a complex and multidisciplinary challenge, requiring a multidisciplinary approach for future solutions.

4. PROSPECTS FOR THE FUTURE

This study has limitations due to budget constraints and the lack of experiments. However, future investigations can potentially address these limitations by incorporating such aspects in developing bone scaffolds. It is imperative that further research be conducted to determine the efficacy of Voronoi tessellation and scaffold design in promoting healing. Non-planar 3D printing methods should be addressed. Additionally, the effectiveness of drug or graft-loaded scaffolds should be evaluated. Material characterization is a necessary step to enhance the quality of future work. Furthermore, prevascularization of bone scaffolds needs further exploration to facilitate optimal healing outcomes.

5. LIST OF PUBLICATIONS PRODUCED FROM THE THESIS

1. Design of Patient-Specific Mandibular Reconstruction Plates and a Hybrid Scaffold Computers in Biology and Medicine S.E.Dogan, C.Ozturk, B.Koc February, 2024

APPENDIX A. SEGMENTATION OF THE TRABECULAR BONE AND RESULTS OF THE FIRST ANALYSIS

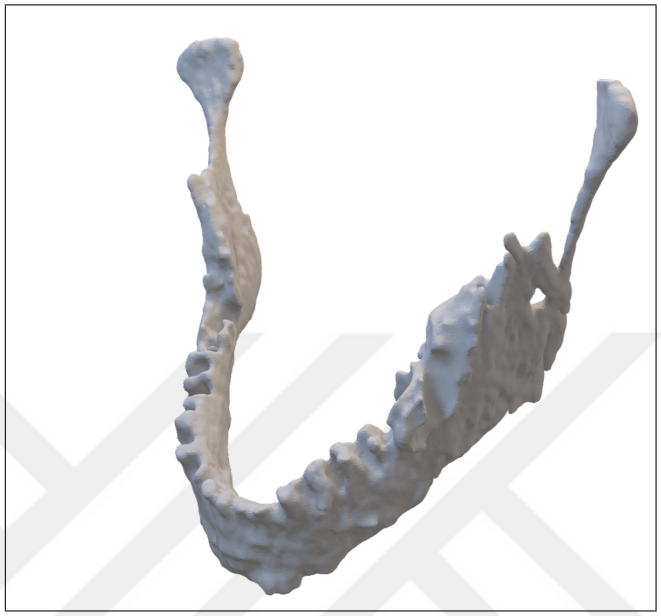

Figure A.1 Segmentation of mandibular trabecular bone.

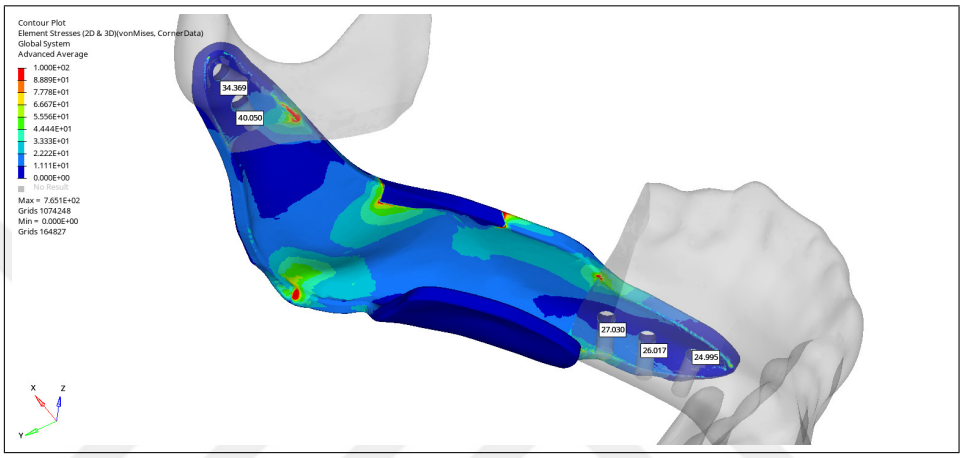

(a)

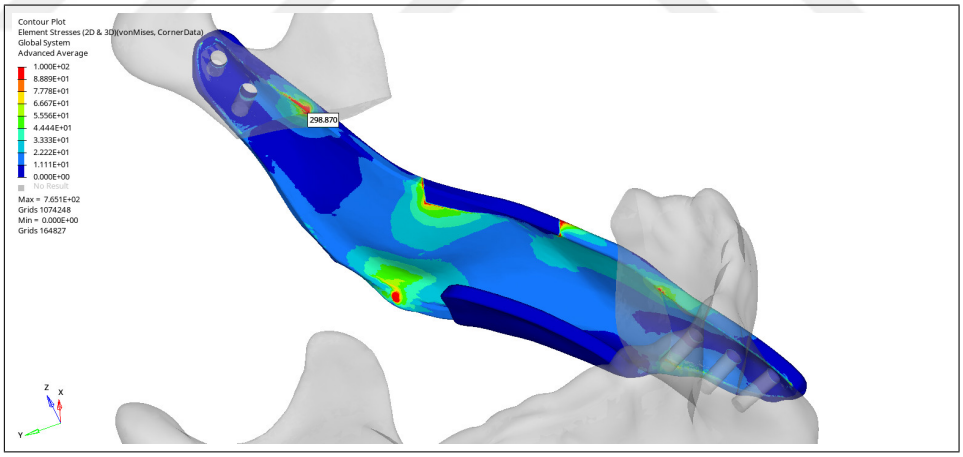

(b)

Figure A.2 Results of the first analysis with constrained left molars. Part 1.

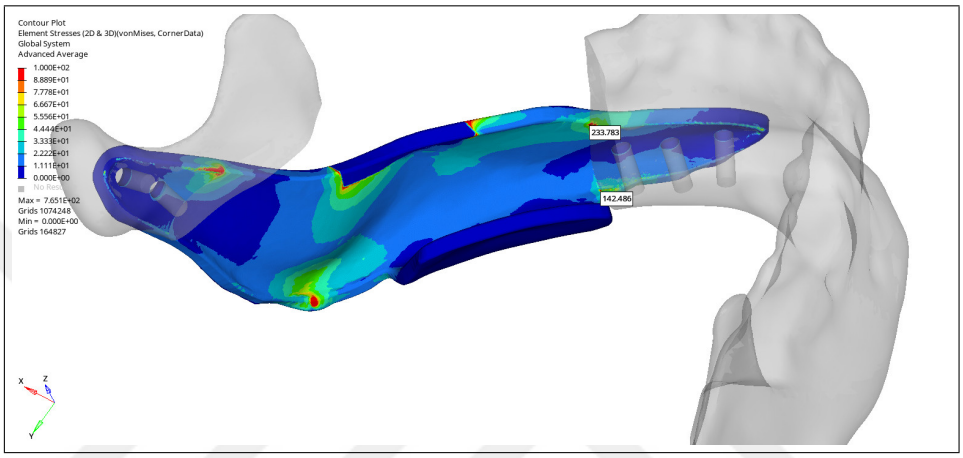

(a)

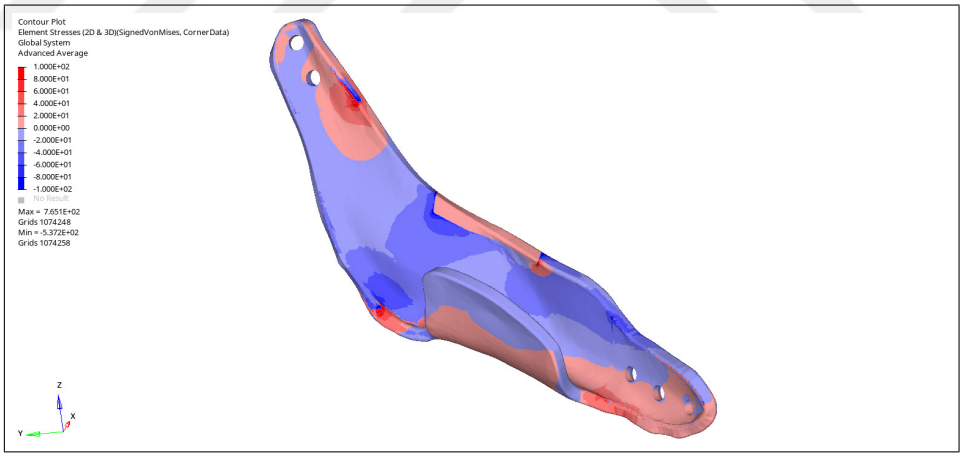

(b)

Figure A.3 Results of the first analysis with constrained left molars. Part 2.

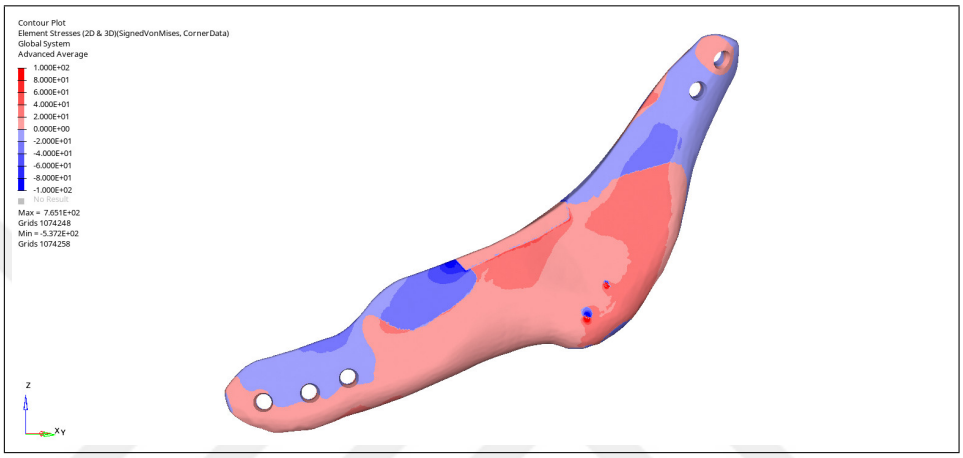

(a)

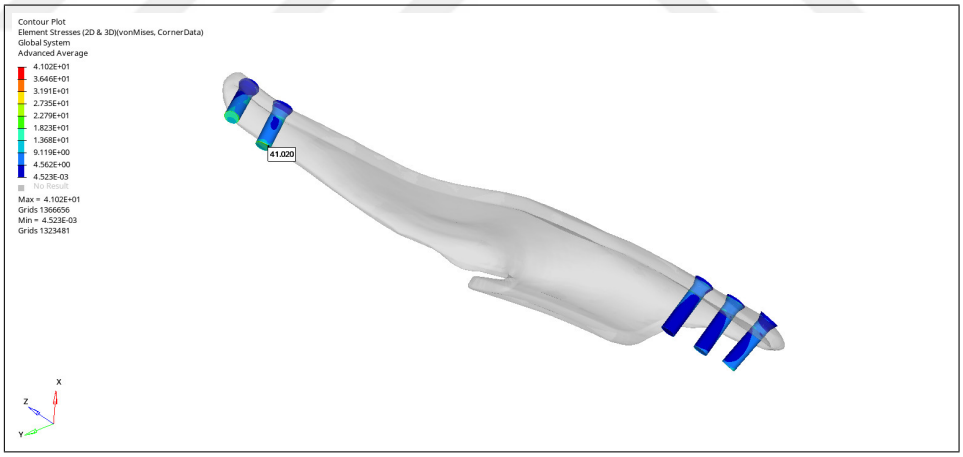

(b)

Figure A.4 Results of the first analysis with constrained left molars. Part 3.

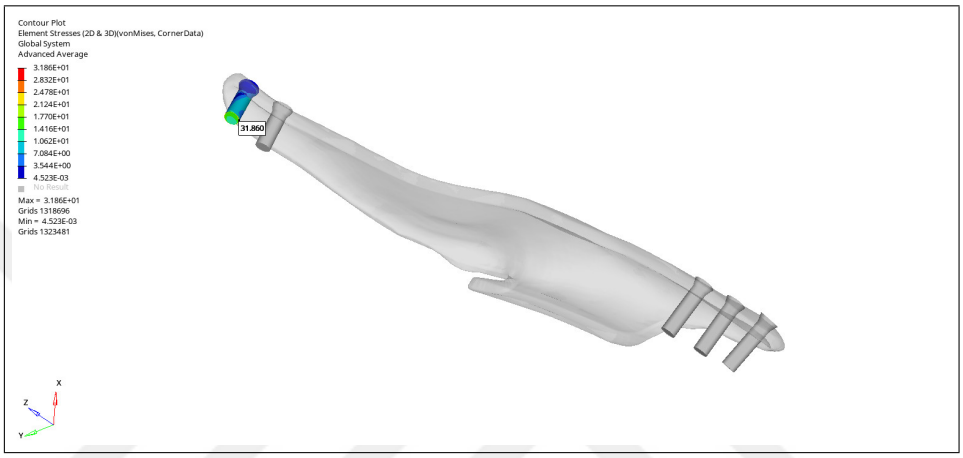

(a)

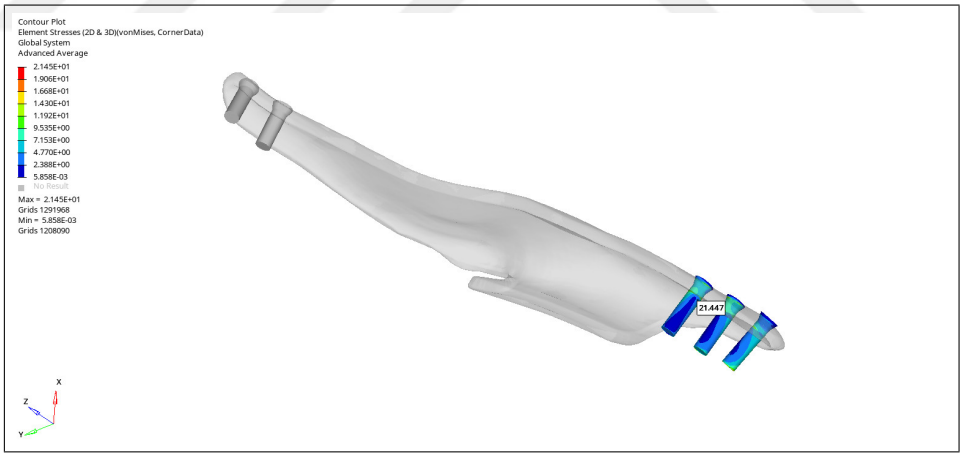

(b)

Figure A.5 Results of the first analysis with constrained left molars. Part 4.

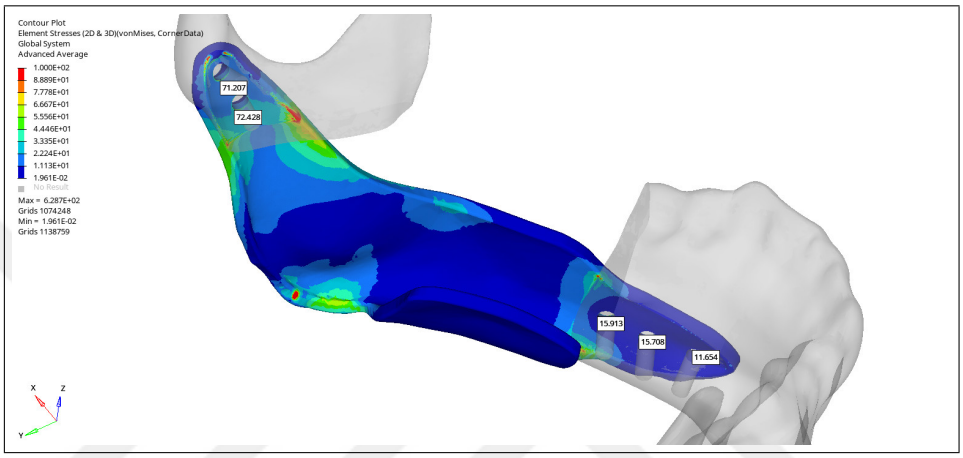

(a)

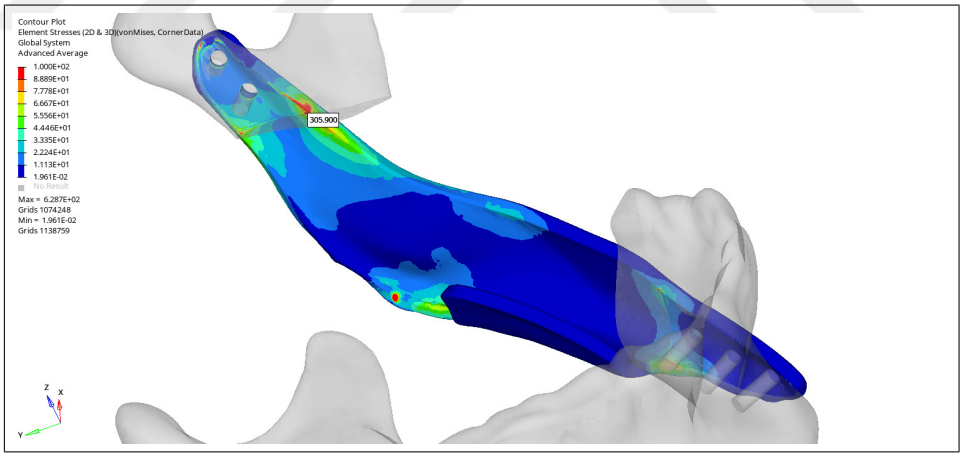

(b)

Figure A.6 Results of the first analysis with constrained right molars. Part 1.

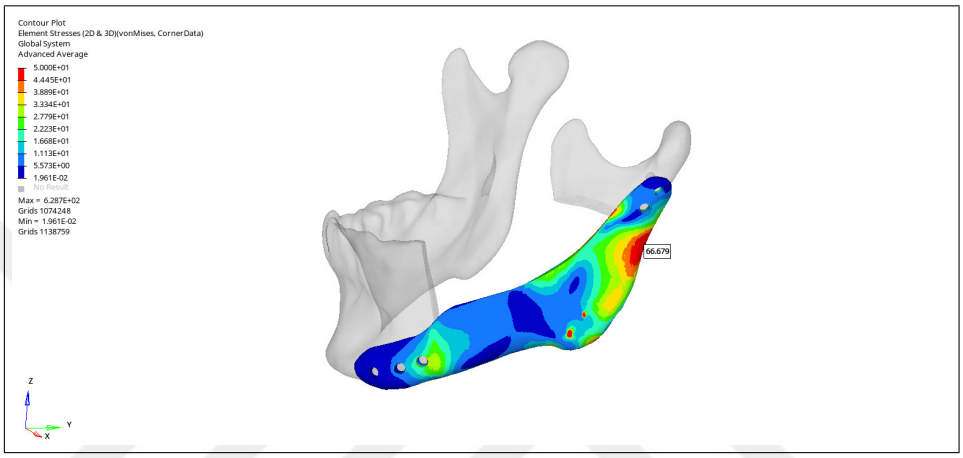

(a)

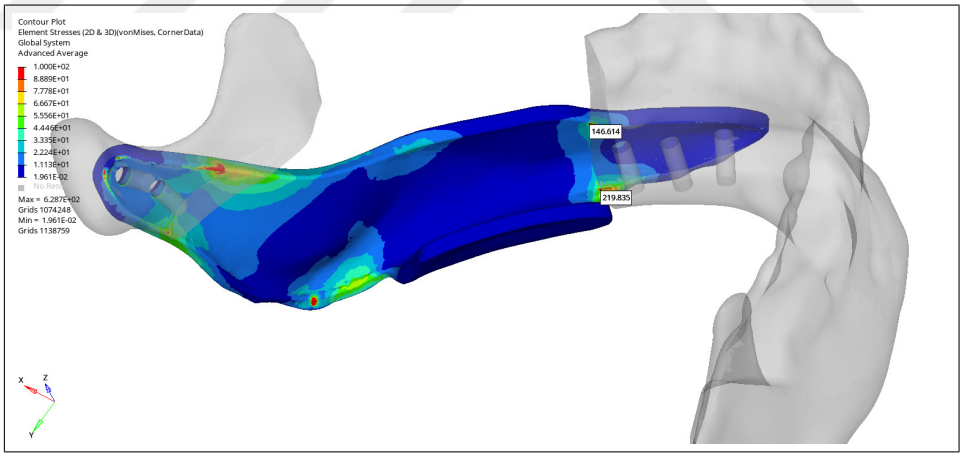

(b)

Figure A.7 Results of the first analysis with constrained right molars. Part 2.

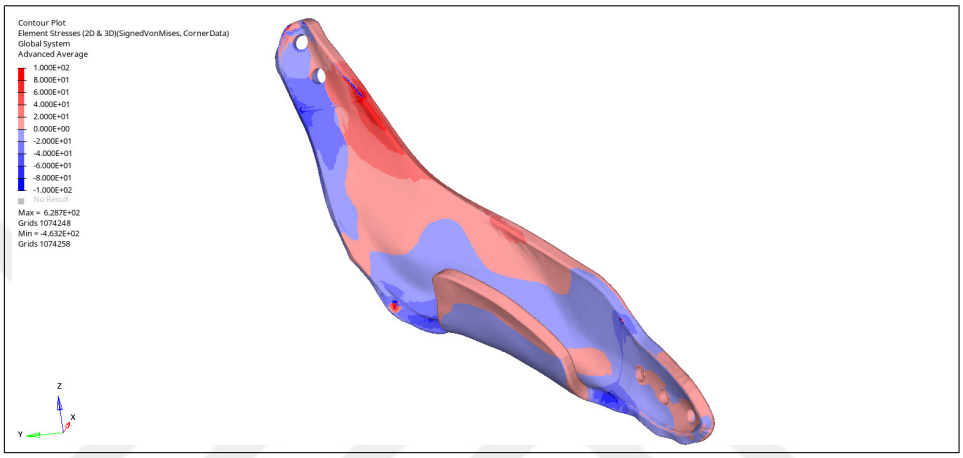

(a)

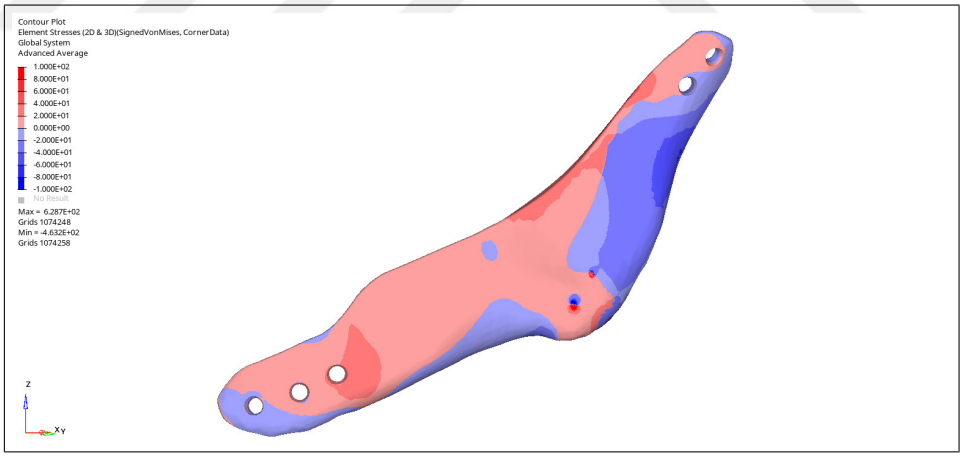

(b)

Figure A.8 Results of the first analysis with constrained right molars. Part 3.

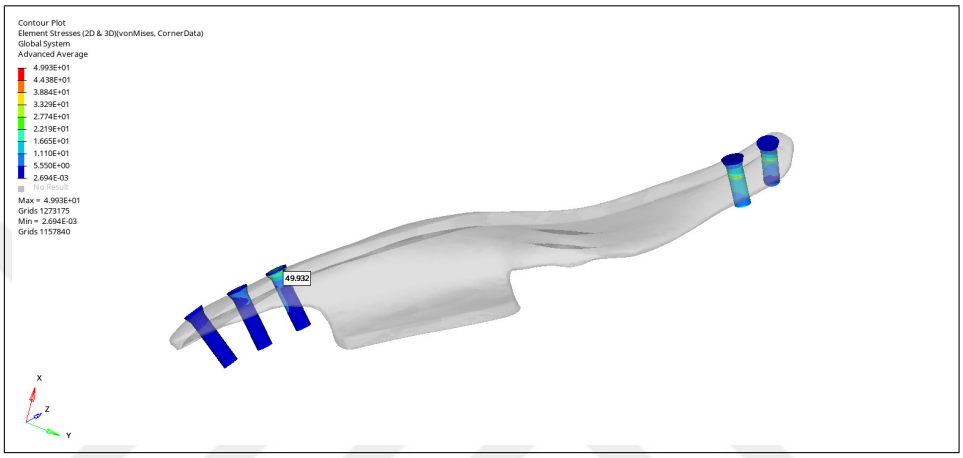

(a)

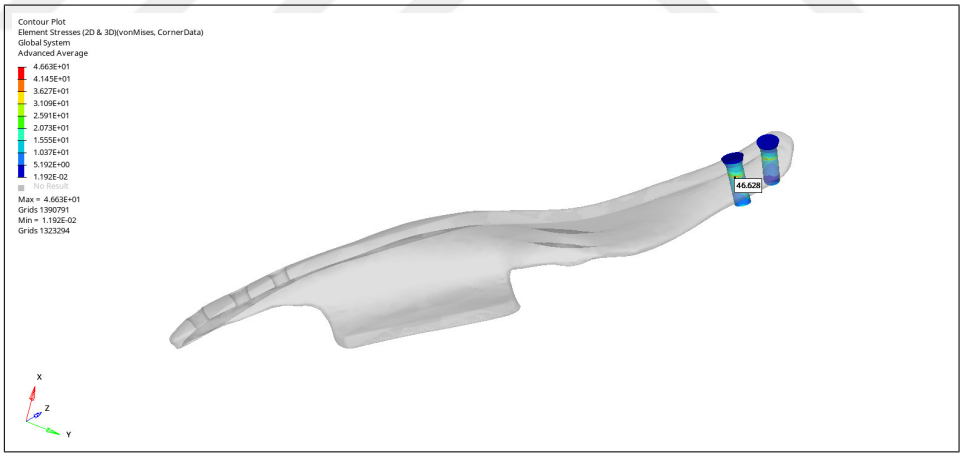

(b)

Figure A.9 Results of the first analysis with constrained right molars. Part 4.

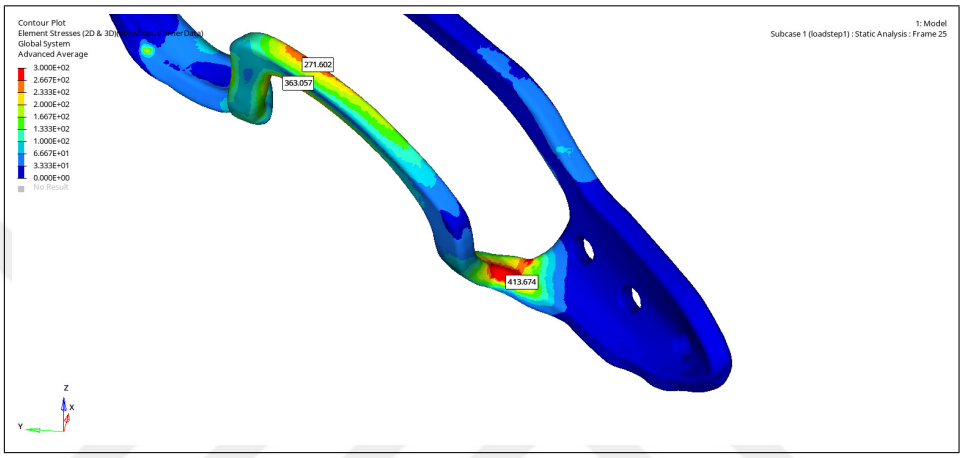

(a)

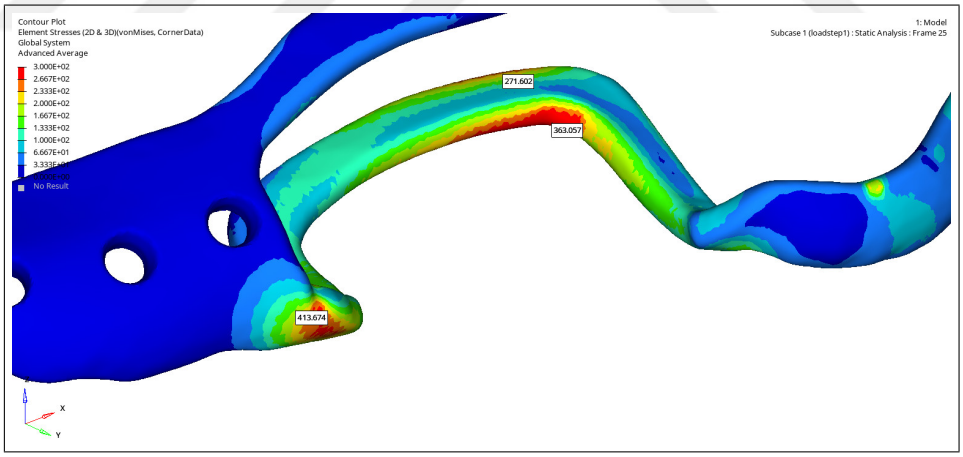

(b)

Figure A.10 Results of the analysis of the hollow plate with constrained molars (left). Part 1.

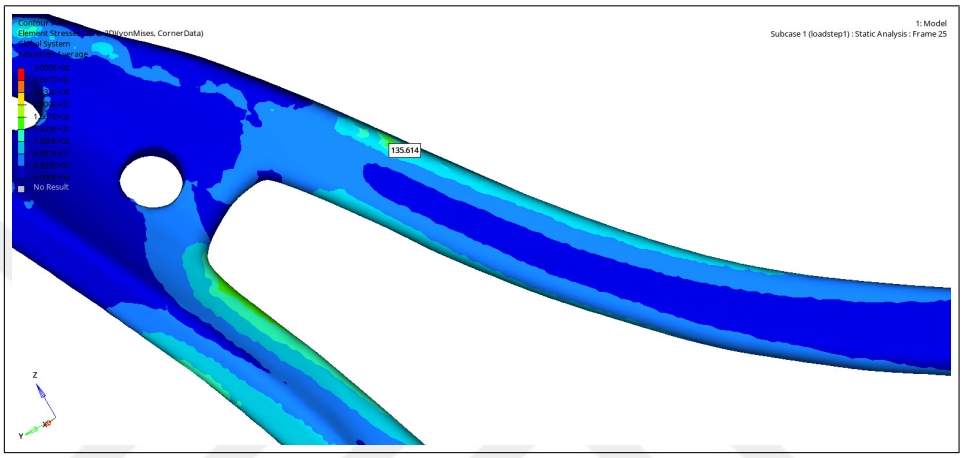

(a)

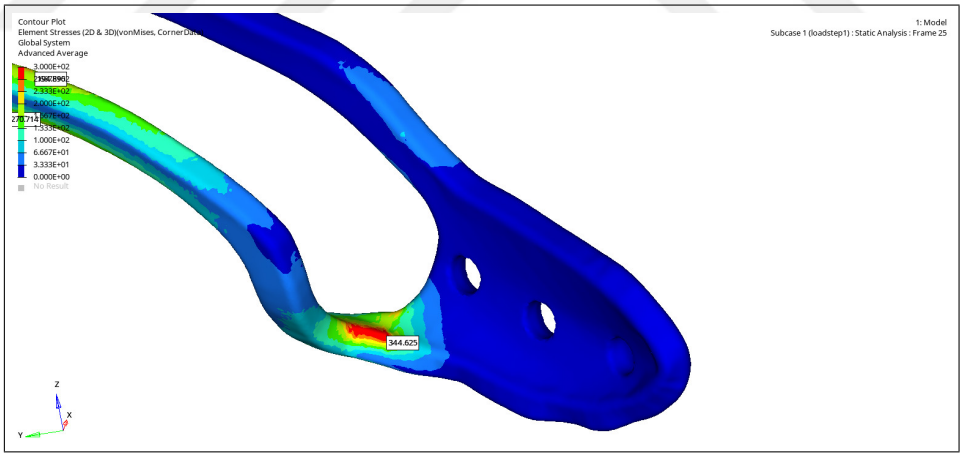

(b)

Figure A.11 Results of the analysis of the hollow plate with constrained molars (right). Part 2.

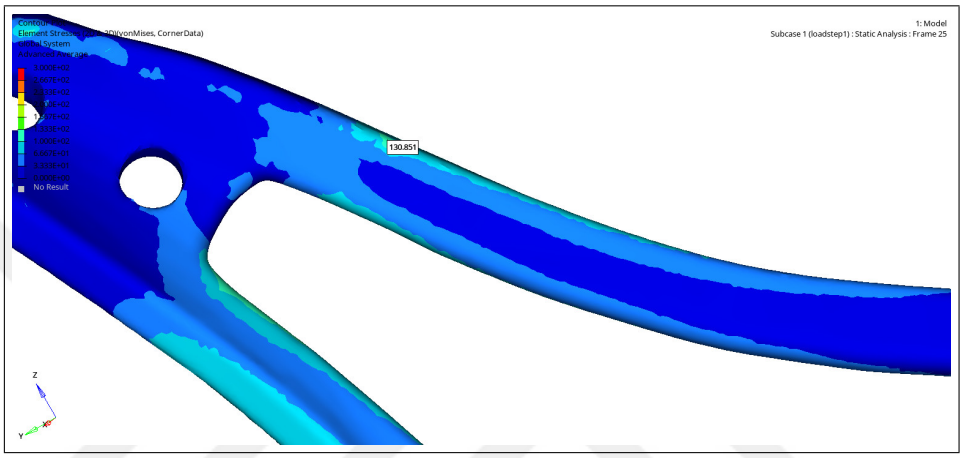

(a)

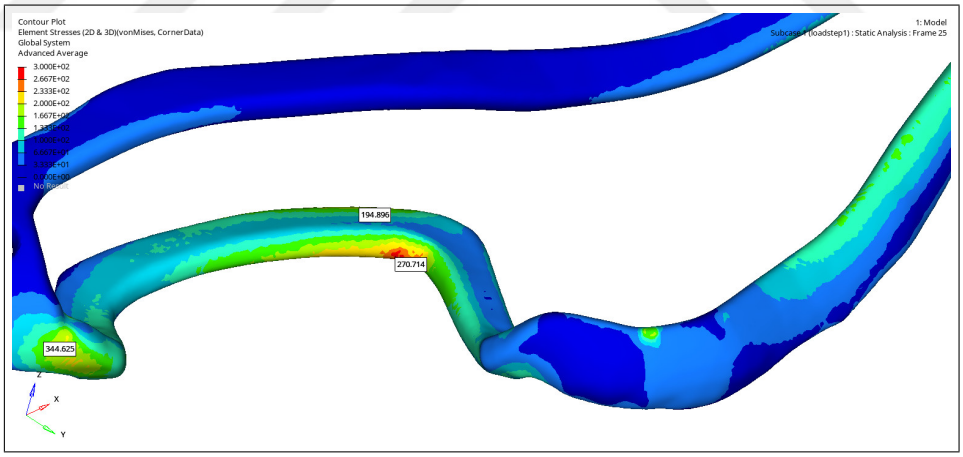

(b)

Figure A.12 Results of the analysis of the hollow plate with constrained molars (right). Part 3.

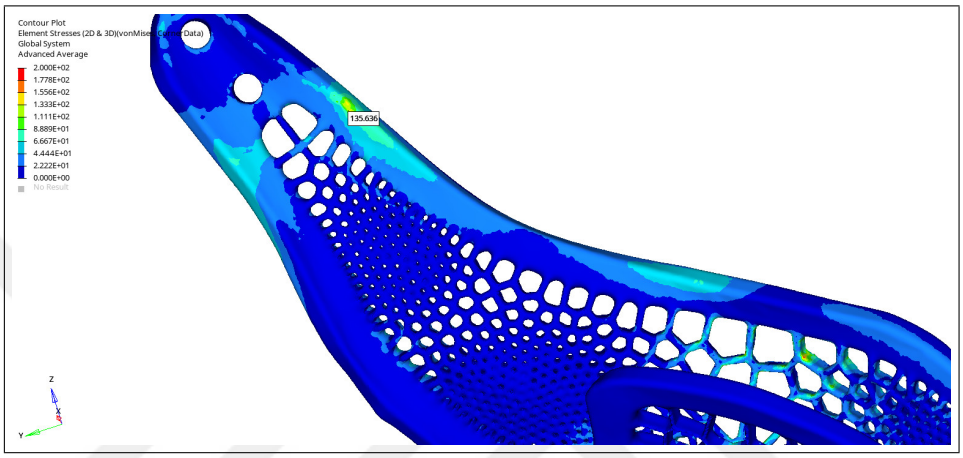

(a)

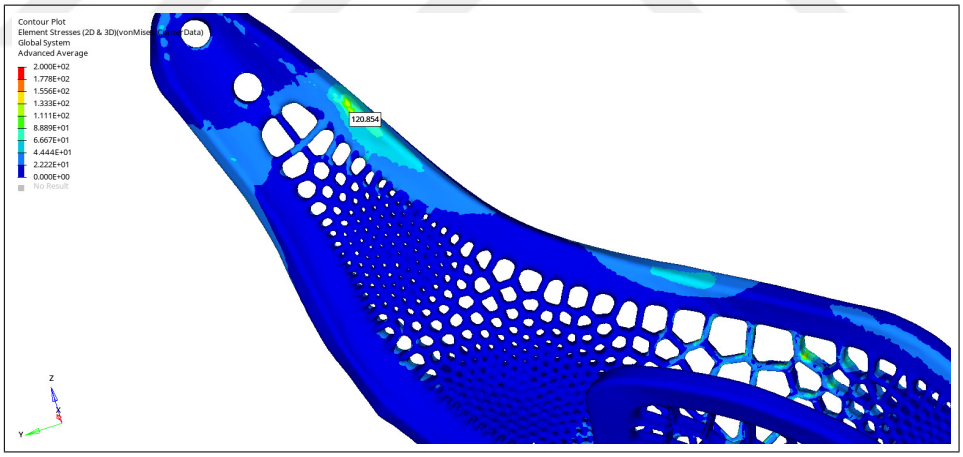

(b)

Figure A.13 Results of the analysis of the Voronoi plate with constrained molars (a: left, b: right). Part 1.

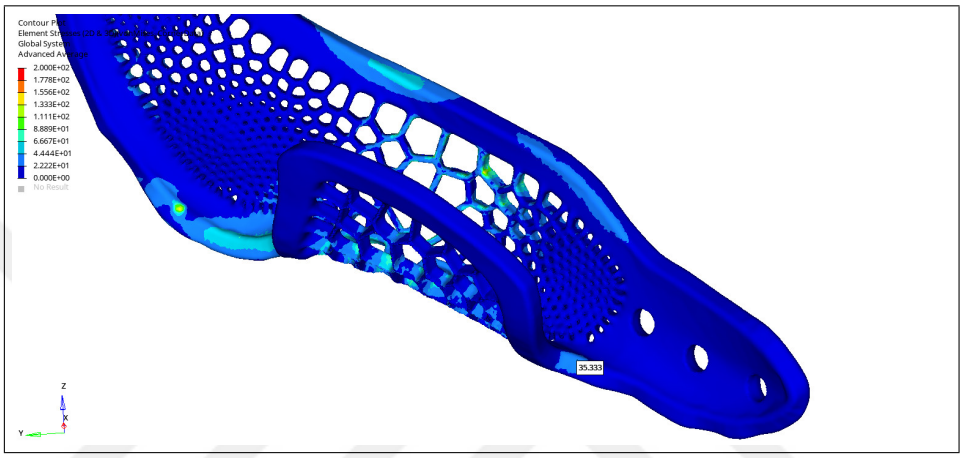

(a)

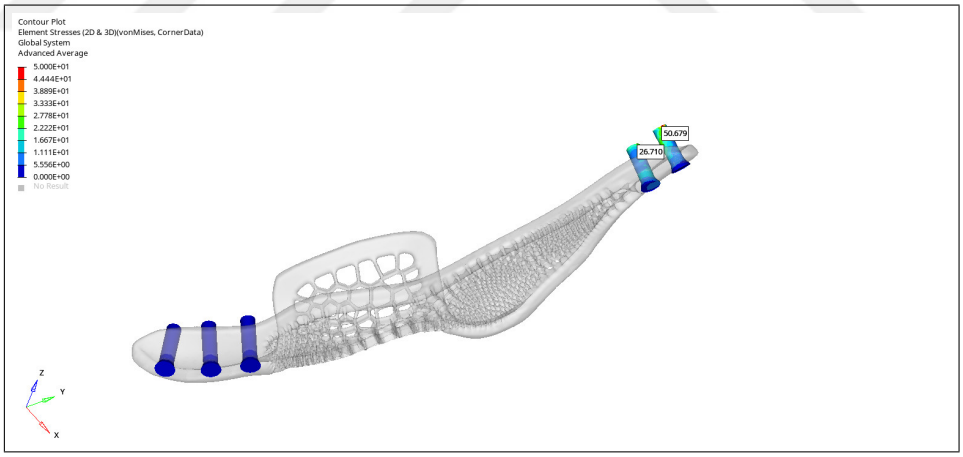

(b)

Figure A.14 Results of the analysis of the Voronoi plate with constrained molars (right). Part 2.

REFERENCES

1. Langer, R., and J. P. Vacanti, "Tissue engineering," *Science*, Vol. 260, pp. 920–926, may 1993.

2. Cordeiro, P. G., P. W. Henderson, and E. Matros, "A 20-year experience with 202 segmental mandibulectomy defects: A defect classification system, algorithm for flap selection, and surgical outcomes," *Plastic &amp Reconstructive Surgery*, Vol. 141, pp. 571e–581e, apr 2018.

3. Koolstra, J., "Dynamics of the human masticatory system," *Critical Reviews in Oral Biology &amp Medicine*, Vol. 13, pp. 366–376, jul 2002.

4. Alford, A. I., D. Nicolaou, M. Hake, and S. McBride-Gagyi, "Masquelet's induced membrane technique: Review of current concepts and future directions," *Journal of Orthopaedic Research*, Vol. 39, pp. 707–718, jan 2021.

5. Hariri, F., S. Y. Chin, and J. Rengarajoo, "Distraction osteogenesis in oral and craniomaxillofacial reconstructive surgery," in *Osteogenesis and Bone Regeneration*, IntechOpen, apr 2019.

6. Sears, N. A., D. R. Seshadri, and P. S. Dhavalikar, "A review of three-dimensional printing in tissue engineering," *Tissue Engineering Part B: Reviews*, Vol. 22, pp. 298–310, aug 2016.

7. Korioth, T. W., and A. G. Hannam, "Mandibular forces during simulated tooth clenching.," *Journal of Oral Facial Pain and Headache*, 1994.

8. Ferneini, E. M., M. T. Goupil, and S. Halepas, eds., *The History of Maxillofacial Surgery*, Springer International Publishing, 2022.

9. Kheirallah, M., and H. Almeshaly, "Present strategies for critical bone defects regeneration," *Oral Health Case Reports*, Vol. 02, no. 03, 2016.

10. "Global, regional, and national burden of 12 mental disorders in 204 countries and territories, 1990–2019: a systematic analysis for the global burden of disease study 2019," *The Lancet Psychiatry*, Vol. 9, pp. 137–150, feb 2022.

11. Aversa, Z., P. Costelli, and M. Muscaritoli, "Cancer-induced muscle wasting: latest findings in prevention and treatment," *Therapeutic Advances in Medical Oncology*, Vol. 9, pp. 369–382, mar 2017.

12. Guise, T. A., "Bone loss and fracture risk associated with cancer therapy," *The Oncologist*, Vol. 11, pp. 1121–1131, nov 2006.

13. Drake, M. T., "Osteoporosis and cancer," *Current Osteoporosis Reports*, Vol. 11, pp. 163–170, jul 2013.

14. Vidal, L., and C. Kampleitner, "Reconstruction of large skeletal defects: Current clinical therapeutic strategies and future directions using 3d printing," *Frontiers in Bioengineering and Biotechnology*, Vol. 8, feb 2020.

15. Merrill, J. P., "Successful homotransplantation of the human kidney between identical twins," *Journal of the American Medical Association*, Vol. 160, p. 277, jan 1956.

16. Mao, A. S., and D. J. Mooney, "Regenerative medicine: Current therapies and future directions," *Proceedings of the National Academy of Sciences*, Vol. 112, pp. 14452–14459, nov 2015.

17. Nikolova, M. P., and M. S. Chavali, "Recent advances in biomaterials for 3d scaffolds: A review," *Bioactive Materials*, Vol. 4, pp. 271–292, dec 2019.

18. Hua, K., I. Rocha, P. Zhang, and S. Gustafsson, "Transition from bioinert to bioactive material by tailoring the biological cell response to carboxylated nanocellulose," *Biomacromolecules*, Vol. 17, pp. 1224–1233, mar 2016.

19. Murphy, S. V., and A. Atala, "3d bioprinting of tissues and organs," *Nature Biotechnology*, Vol. 32, pp. 773–785, aug 2014.

20. Ozbolat, I. T., *3D Bioprinting*, Elsevier, 2017.

21. Ko, E. W.-C., T. T.-Y. Teng, and C. S. Huang, "The effect of early physiotherapy on the recovery of mandibular function after orthognathic surgery for class III correction. part II: Electromyographic activity of masticatory muscles," *Journal of Cranio-Maxillofacial Surgery*, Vol. 43, pp. 138–143, jan 2015.

22. Yang, H. J., I. J. Kwon, and A. A. Almansoori, "Effects of chewing exerciser on the recovery of masticatory function recovery after orthognathic surgery: A single-center randomized clinical trial, a preliminary study," *Medicina*, Vol. 56, p. 483, sep 2020.

23. Navarro-Fernández, G., and A. Gil-Martínez, "Effectiveness of physical therapy in orthognathic surgery patients: A systematic review of randomized controlled trials," *Journal of Functional Morphology and Kinesiology*, Vol. 8, p. 17, jan 2023.

24. de Graeff, A., J. de Leeuw, W. Ros, and G. Hordijk, "A prospective study on quality of life of patients with cancer of the oral cavity or oropharynx treated with surgery with or without radiotherapy," *Oral Oncology*, Vol. 35, pp. 27–32, jan 1999.

25. Rogers, S. N., J. Devine, and D. Lowe, "Longitudinal health-related quality of life after mandibular resection for oral cancer: a comparison between rim and segment," *Head &amp Neck*, Vol. 26, pp. 54–62, jan 2004.

26. Hidalgo, D. A., "Fibula free flap," *Plastic and Reconstructive Surgery*, Vol. 84, pp. 71–79, jul 1989.

27. Hazrati, E., "A comparison of vascularized and nonvascularized bone grafts for reconstruction of mandibular continuity defects.," *Plastic &amp Reconstructive Surgery*, Vol. 104, p. 1591, oct 1999.

28. Paré, A., A. Bossard, and B. Laure, "Reconstruction of segmental mandibular defects: Current procedures and perspectives," *Laryngoscope Investigative Otolaryngology*, Vol. 4, pp. 587–596, nov 2019.

29. van Gemert, J. T., and R. J. van Es, "Free vascularized flaps for reconstruction of the mandible: Complications, success, and dental rehabilitation," *Journal of Oral and Maxillofacial Surgery*, Vol. 70, pp. 1692–1698, jul 2012.

30. Chang, Y.-M., E. Santamaria, F.-C. Wei, and H.-C. Chen, "Primary insertion of osseointegrated dental implants into fibula osteoseptocutaneous free flap for mandible reconstruction," *Plastic and Reconstructive Surgery*, Vol. 102, pp. 680–688, sep 1998.

31. Blackwell, K. E., D. Buchbinder, and M. L. Urken, "Lateral mandibular reconstruction using soft-tissue free flaps and plates," *Archives of Otolaryngology - Head and Neck Surgery*, Vol. 122, pp. 672–678, jun 1996.

32. Lin, J. A.-J., "Free flap outcomes of microvascular reconstruction after repeated segmental mandibulectomy in head and neck cancer patients," *Scientific Reports*, Vol. 9, may 2019.

33. Hoit, G., M. S. Kain, and J. W. Sparkman, "The induced membrane technique for bone defects: Basic science, clinical evidence, and technical tips," *OTA International: The Open Access Journal of Orthopaedic Trauma*, Vol. 4, p. e106, apr 2021.

34. Masquelet, A.-C., M. B. maitigue, and T. Bégué, "Reconstruction diaphysaire par membrane induite, greffe spongieuse et BMP," *Revue de Chirurgie Orthopédique et Réparatrice de l'Appareil Moteur*, Vol. 92, pp. 518–519, sep 2006.

35. Yüceer-Çetiner, E., N. Özkan, and M. E. Önger, "Is induced membrane technique effective in reconstruction of mandibular segmental bone defects? an experimental study," *Journal of Cranio-Maxillofacial Surgery*, Vol. 49, pp. 1130–1140, dec 2021.

36. Brookes, C., "Induced membranes for segmental mandibular reconstruction: technique review and case series," *International Journal of Oral and Maxillofacial Surgery*, Vol. 48, p. 135, may 2019.

37. Liantis, P., A. F. Mavrogenis, and N. A. Stavropoulos, "Risk factors for and complications of distraction osteogenesis," *European Journal of Orthopaedic Surgery &amp Traumatology*, Vol. 24, pp. 693–698, jun 2013.

38. Mah, M. C., *Functional outcomes and long term complications following distraction osteogenesis of the maxilla and mandible : a systematic review.* PhD thesis.

39. Stucki-McCormick, S. U., and L. F. Clarizio, "Complications associated with distraction osteogenesis," in *Complications in Cranio-Maxillofacial and Oral Surgery*, pp. 49–69, Springer International Publishing, 2020.

40. Primrose, A., E. Broadfoot, P. Diner, and F. M. and, "Patients' responses to distraction osteogenesis: a multi-centre study," *International Journal of Oral and Maxillofacial Surgery*, Vol. 34, pp. 238–242, may 2005.

41. Prasadh, S., and R. C. W. Wong, "Unraveling the mechanical strength of biomaterials used as a bone scaffold in oral and maxillofacial defects," *Oral Science International*, Vol. 15, pp. 48–55, apr 2018.

42. Wong, S. K., M. M. F. Yee, and K.-Y. Chin, "A review of the application of natural and synthetic scaffolds in bone regeneration," *Journal of Functional Biomaterials*, Vol. 14, p. 286, may 2023.

43. Zha, Y., Y. Li, T. Lin, J. Chen, and S. Zhang, "Progenitor cell-derived exosomes endowed with VEGF plasmids enhance osteogenic induction and vascular remodeling in large segmental bone defects," *Theranostics*, Vol. 11, no. 1, pp. 397–409, 2021.

44. Mondal, S., and U. Pal, "3d hydroxyapatite scaffold for bone regeneration and local drug delivery applications," *Journal of Drug Delivery Science and Technology*, Vol. 53, p. 101131, oct 2019.

45. Tampieri, A., E. Landi, F. Valentini, M. Sandri, and T. D'Alessandro, "A conceptually new type of bio-hybrid scaffold for bone regeneration," *Nanotechnology*, Vol. 22, p. 015104, dec 2010.

46. Gkioni, C., S. Leeuwenburgh, and J. Jansen, "Bone tissue engineering: Biodegradable polymeric–ceramic composite scaffolds for tissue regeneration," in *Encyclopedia of Biomedical Polymers and Polymeric Biomaterials*, pp. 1148–1163, Taylor & Francis, jan 2016.

47. Filippi, M., G. Born, M. Chaaban, and A. Scherberich, "Natural polymeric scaffolds in bone regeneration," *Frontiers in Bioengineering and Biotechnology*, Vol. 8, may 2020.

48. Donnaloja, F., E. Jacchetti, M. Soncini, and M. T. Raimondi, "Natural and synthetic polymers for bone scaffolds optimization," *Polymers*, Vol. 12, p. 905, apr 2020.

49. Bhattarai, D., L. Aguilar, C. Park, and C. Kim, "A review on properties of natural and synthetic based electrospun fibrous materials for bone tissue engineering," *Membranes*, Vol. 8, p. 62, aug 2018.

50. Donate, R., M. Monzón, and M. E. Alemán-Domínguez, "Additive manufacturing of PLA-based scaffolds intended for bone regeneration and strategies to improve their biological properties," *e-Polymers*, Vol. 20, pp. 571–599, jan 2020.

51. "A pH-triggered, self-assembled, and bioprintable hybrid hydrogel scaffold for mesenchymal stem cell based bone tissue engineering."

52. Xue, J., *A bioinspired three-dimensional graphene/chitosan hybrid scaffold for bone tissue engineering.* PhD thesis.

53. "Nanostructured surface bioactive composite scaffold for filling of bone defects," *Biointerface Research in Applied Chemistry*, Vol. 10, pp. 5038–5047, jan 2020.

54. Shao, H., J. He, T. Lin, Z. Zhang, and Y. Zhang, "3d gel-printing of hydroxyapatite scaffold for bone tissue engineering," *Ceramics International*, Vol. 45, pp. 1163–1170, jan 2019.

55. "A biomimetic macroporous hybrid scaffold with sustained drug delivery for enhanced bone regeneration."

56. Nandakumar, A., A. Barradas, J. de Boer, and L. Moroni, "Combining technologies to create bioactive hybrid scaffolds for bone tissue engineering," *Biomatter*, Vol. 3, p. e23705, apr 2013.

57. Amiryaghoubi, N., N. N. Pesyan, and M. Fathi, "Injectable thermosensitive hybrid hydrogel containing graphene oxide and chitosan as dental pulp stem cells scaffold for bone tissue engineering," *International Journal of Biological Macromolecules*, Vol. 162, pp. 1338–1357, nov 2020.

58. Kim, H.-W., J. C. Knowles, and H.-E. Kim, "Hydroxyapatite/poly(-caprolactone) composite coatings on hydroxyapatite porous bone scaffold for drug delivery," *Biomaterials*, Vol. 25, pp. 1279–1287, mar 2004.

59. Oliveira, J. M., M. T. Rodrigues, and S. S. Silva, "Novel hydroxyapatite/chitosan bilayered scaffold for osteochondral tissue-engineering applications: Scaffold design and its performance when seeded with goat bone marrow stromal cells," *Biomaterials*, Vol. 27, pp. 6123–6137, dec 2006.

60. Torgbo, S., and P. Sukyai, "Fabrication of microporous bacterial cellulose embedded with magnetite and hydroxyapatite nanocomposite scaffold for bone tissue engineering," *Materials Chemistry and Physics*, Vol. 237, p. 121868, nov 2019.

61. Yin, S., W. Zhang, Z. Zhang, and X. Jiang, "Recent advances in scaffold design and material for vascularized tissue-engineered bone regeneration," *Advanced Healthcare Materials*, Vol. 8, apr 2019.

62. Yang, Y., L. Chu, S. Yang, and H. Zhang, "Dual-functional 3d-printed composite scaffold for inhibiting bacterial infection and promoting bone regeneration in infected bone defect models," *Acta Biomaterialia*, Vol. 79, pp. 265–275, oct 2018.

63. El-Fiqi, A., J.-H. Kim, and H.-W. Kim, "Novel bone-mimetic nanohydroxyapatite/collagen porous scaffolds biomimetically mineralized from surface silanized mesoporous nanobioglass/collagen hybrid scaffold: Physicochemical, mechanical and in vivo evaluations," *Materials Science and Engineering: C*, Vol. 110, p. 110660, may 2020.

64. Kim, S. E., and A. P. Tiwari, "Three dimensional polycaprolactone/cellulose scaffold containing calcium-based particles: a new platform for bone regeneration," *Carbohydrate Polymers*, Vol. 250, p. 116880, dec 2020.

65. Singh, B., N. Panda, R. Mund, and K. Pramanik, "Carboxymethyl cellulose enables silk fibroin nanofibrous scaffold with enhanced biomimetic potential for bone tissue engineering application," *Carbohydrate Polymers*, Vol. 151, pp. 335–347, oct 2016.

66. Wei, L., S. Wu, M. Kuss, X. Jiang, and R. Sun, "3d printing of silk fibroin-based hybrid scaffold treated with platelet rich plasma for bone tissue engineering," *Bioactive Materials*, Vol. 4, pp. 256–260, dec 2019.

67. Lourenço, A. H., and A. L. Torres, "Osteogenic, anti-osteoclastogenic and immunomodulatory properties of a strontium-releasing hybrid scaffold for bone repair," *Materials Science and Engineering: C*, Vol. 99, pp. 1289–1303, jun 2019.

68. Mohammadi, M., M. Alibolandi, K. Abnous, and Z. Salmasi, "Fabrication of hybrid scaffold based on hydroxyapatite-biodegradable nanofibers incorporated with liposomal formulation of BMP-2 peptide for bone tissue engineering," *Nanomedicine: Nanotechnology, Biology and Medicine*, Vol. 14, pp. 1987–1997, oct 2018.

69. Raucci, M. G., C. Demitri, and A. Soriente, "Gelatin/nano-hydroxyapatite hydrogel scaffold prepared by sol-gel technology as filler to repair bone defects," *Journal of Biomedical Materials Research Part A*, Vol. 106, pp. 2007–2019, apr 2018.

70. Shrestha, B. K., S. Shrestha, and A. P. Tiwari, "Bio-inspired hybrid scaffold of zinc oxide-functionalized multi-wall carbon nanotubes reinforced polyurethane nanofibers for bone tissue engineering," *Materials &amp Design*, Vol. 133, pp. 69–81, nov 2017.

71. Abbasian, V., R. Emadi, and M. Kharaziha, "Biomimetic nylon 6-baghdadite nanocomposite scaffold for bone tissue engineering," *Materials Science and Engineering: C*, Vol. 109, p. 110549, apr 2020.

72. Feng, P., P. Wu, C. Gao, Y. Yang, and W. Guo, "A multimaterial scaffold with tunable properties: Toward bone tissue repair," *Advanced Science*, Vol. 5, apr 2018.

73. Yushkevich, P. A., J. Piven, C. Hazlett, and S. Ho, "User-guided 3D active contour segmentation of anatomical structures: Significantly improved efficiency and reliability," *Neuroimage*, Vol. 31, no. 3, pp. 1116–1128, 2006.

74. Pankert, T., H. Lee, F. Peters, and F. Hölzle, "Mandible segmentation from CT data for virtual surgical planning using an augmented two-stepped convolutional neural network," *International Journal of Computer Assisted Radiology and Surgery*, Vol. 18, pp. 1479–1488, jan 2023.

75. Singh, G., B. Harjani, R. Singh, and U. Pal, "Locking v/s non-locking reconstruction plates in mandibular reconstruction," *National Journal of Maxillofacial Surgery*, Vol. 3, no. 2, p. 159, 2012.

76. Rotaru, "In vivo behavior of surface modified ti6al7nb alloys used in selective laser melting for custom-made implants. a preliminary study," in *54(3 Suppl), 791–796*, Romanian journal of morphology and embryology = Revue roumaine de morphologie et embryologie, 2013.

77. Zhang, L.-C., and L.-Y. Chen, "A review on biomedical titanium alloys: Recent progress and prospect," *Advanced Engineering Materials*, Vol. 21, mar 2019.

78. Bolzoni, L., E. Ruiz-Navas, E. Neubauer, and E. Gordo, "Mechanical properties and microstructural evolution of vacuum hot-pressed titanium and ti–6al–7nb alloy," *Journal of the Mechanical Behavior of Biomedical Materials*, Vol. 9, pp. 91–99, may 2012.

79. Benady, A., S. J. Meyer, E. Golden, and S. Dadia, "Patient-specific ti-6al-4v lattice implants for critical-sized load-bearing bone defects reconstruction," *Materials &amp Design*, Vol. 226, p. 111605, feb 2023.

80. Dutta, A., K. Mukherjee, S. Dhara, and S. Gupta, "Design of porous titanium scaffold for complete mandibular reconstruction: The influence of pore architecture parameters," *Computers in Biology and Medicine*, Vol. 108, pp. 31–41, may 2019.

81. Hijazi, L., W. Hejazi, M. A. Darwich, and K. Darwich, "Finite element analysis of stress distribution on the mandible and condylar fracture osteosynthesis during various clenching tasks," *Oral and Maxillofacial Surgery*, Vol. 20, pp. 359–367, sep 2016.

82. Lakatos, É., L. Magyar, and I. Bojtár, "Material properties of the mandibular trabecular bone," *Journal of Medical Engineering*, Vol. 2014, pp. 1–7, oct 2014.

83. An, Y. H., and R. A. Draughn, eds., *Mechanical Testing of Bone and the Bone-Implant Interface*, CRC Press, nov 1999.

84. Kang, J., J. Zhang, J. Zheng, and L. Wang, "3d-printed PEEK implant for mandibular defects repair - a new method," *Journal of the Mechanical Behavior of Biomedical Materials*, Vol. 116, p. 104335, apr 2021.

85. Zhao, H., Y. Han, C. Pan, and D. Yang, "Design and mechanical properties verification of gradient voronoi scaffold for bone tissue engineering," *Micromachines*, Vol. 12, p. 664, jun 2021.

86. Sharma, N., D. Ostas, and H. Rotar, "Design and additive manufacturing of a biomimetic customized cranial implant based on voronoi diagram," *Frontiers in Physiology*, Vol. 12, apr 2021.

87. Deering, J., K. I. Dowling, and L.-A. DiCecco, "Selective voronoi tessellation as a method to design anisotropic and biomimetic implants," *Journal of the Mechanical Behavior of Biomedical Materials*, Vol. 116, p. 104361, apr 2021.

88. Koç, B., "Bone bricks: The effect of architecture and material composition on the mechanical and biological performance of bone scaffolds."

89. Zhang, F., C. C. Peck, and A. G. Hannam, "Mass properties of the human mandible," *Journal of Biomechanics*, 2002.

90. Gutwald, R., R. Jaeger, and F. M. Lambers, "Customized mandibular reconstruction plates improve mechanical performance in a mandibular reconstruction model," *Computer Methods in Biomechanics and Biomedical Engineering*, 2016.

91. Koshy, J., E. Feldman, C. Chike-Obi, and J. Bullocks, "Pearls of mandibular trauma management," *Seminars in Plastic Surgery*, 2010.

92. Park, S.-M., S. Park, J. Park, and M. Choi, "Design process of patient-specific osteosynthesis plates using topology optimization," *Journal of Computational Design and Engineering*, 2021.

93. Koper, D. C., C. A. Leung, and L. C. Smeets, "Topology optimization of a mandibular reconstruction plate and biomechanical validation," *Journal of the Mechanical Behavior of Biomedical Materials*, 2021.

94. Krishani, M., W. Y. Shin, H. Suhaimi, and N. S. Sambudi, "Development of scaffolds from bio-based natural materials for tissue regeneration applications: A review," *Gels*, 2023.

95. Chan, B. P., and K. W. Leong, "Scaffolding in tissue engineering: general approaches and tissue-specific considerations," *European Spine Journal*, 2008.

96. Suamte, L., A. Tirkey, J. Barman, and P. J. Babu, "Various manufacturing methods and ideal properties of scaffolds for tissue engineering applications," *Smart Materials in Manufacturing*, 2023.

97. Wang, M., *Materials Selection and Scaffold Fabrication for Tissue Engineering in Orthopaedics*, pp. 259–288. Berlin, Heidelberg: Springer Berlin Heidelberg, 2007.

98. Niu, Y., L. Chen, and T. Wu, "Recent advances in bioengineering bone revascularization based on composite materials comprising hydroxyapatite," *International Journal of Molecular Sciences*, 2023.

99. Abbasi, N., S. Hamlet, R. M. Love, and N.-T. Nguyen, "Porous scaffolds for bone regeneration," *Journal of Science: Advanced Materials and Devices*, Vol. 5, no. 1, pp. 1–9, 2020.